Homogenization: Theories and Applications

M2R Project

Group 9
Supervisor: Dr. Arianna Giunti

Imperial College London

2022/06

Contents

1 Introduction

Homogenization is, in essence, understanding how microscopic behaviour influences macroscopic behaviour. It can be found in many real-world problems, such as conductivity, electricity and turbulence. While it is difficult to analyze many materials and fields on a microscale level due to interactive complexity, it is observed that many such physical properties exhibit some homogeneity on a macroscale. Our goal is to model the microscale behaviour using a family of partial differential equations indexed by ε, the spatial scale parameter, and derive a simplified partial differential equation by studying the limit as ε tends to 0. Throughout this report, we focus on the equation $-\nabla \cdot (A(x, \frac{x}{\varepsilon})\nabla u_\varepsilon) = f$. We will first explore the one-dimensional case, which is divided further into periodic and stochastic $A(x, \frac{x}{\varepsilon})$. After that, we dive deeper into a more general n-dimensional setting, where we will utilize the energy method (the oscillating test function method), a general method for testing the convergence of sequences of functions developed by Tartar[11],[12],[13]. We then move our focus to applications, where we use two different approaches - Iterative Stencil Loop and Relaxation Method - to provide numerical intuition of homogenization. We finish by applying the theories developed to 2-dimensional periodic, layered and stochastic media and investigate the effect of variations on the homogenized parameters.

2 Theories in 1-D model

We will consider the problem in the context of heat conductivity.
Consider a heat-conducting rod in one dimension occupying the domain $O = (0, L) \subset \mathbb{R}$. Suppose the rod is exposed to a heat source/sink that does not vary in time, with Dirichlet boundary condition that the temperature of the rod is 0 for all time at the boundary. We consider the steady-state limit of the temperature evolution (i.e., temperature is independent of time, so $\partial_t u = 0$), which can be described by the boundary value problem

$$\begin{aligned} -\partial_x(a\partial_x u) &= f \qquad \text{in} \quad O, \\ u &= 0 \qquad \text{on} \quad \partial O. \end{aligned} \tag{1}$$

where

$u(x) : O \to \mathbb{R}$ denotes the temperature of the rod
$f(x) : O \to \mathbb{R}$ denotes the known equation describing the heat source/sink
$a(x) : O \to \mathbb{R}^+$ denotes the conductivity of the material

The material of the rod is *homogeneous* if $a(x)$ is constant, and *heterogeneous* otherwise. We will be focusing on the heterogeneous case. In particular, we will be studying heterogeneous materials with microstructure, which means the heterogeneity varies on the microscale l, which is much smaller (ratio $\lesssim 10^{-3}$) than the macroscale. In the one-dimensional case, we denote the macroscale to be the length of the rod L.
Denote ε to be the ratio $\frac{l}{L}$. The goal of homogenization is to derive a simplified PDE by studying the limit $\varepsilon \to 0$.

2.1 Periodic

The main results of this section are from Stefan Neukamm's lecture notes [8].
In this section, we focus on the case where $a(x)$ is periodic with period l, i.e., $a(x) = a_0(\frac{x}{l})$, where a_0 has period 1. Consider a family of functions u_ε, $\varepsilon > 0$. For a fixed ε, let u_ε be the solution to (1) with $a_\varepsilon(x) = a(\frac{x}{\varepsilon})$, where a is 1-periodic and uniformly elliptic, i.e., $\exists \lambda > 0 \;\; s.t. \;\; a(x) \in (\lambda, 1) \;\; \forall x \in \mathbb{R}$. In other words, u_ε is the solution to the equation

$$\begin{cases} -\partial_x \left(a\left(\frac{x}{\varepsilon}\right)\partial_x u_\varepsilon(x)\right) = f & \text{in } O \\ u_\varepsilon = 0 & \text{on } \partial O \end{cases} \tag{2}$$

2.1.1 Existence and Uniqueness

In this section, we prove that $\forall \varepsilon > 0$, $\exists$ a unique smooth solution to (2).

Lemma 2.1. *(Existence and uniqueness of u_ε)*

Consider (2) with assumptions:

1. a: $\mathbb{R} \to \mathbb{R}$ is 1-periodic

2. a is uniformly elliptic, i.e., $\exists \lambda > 0$ such that $a(x) \in (\lambda, 1)$, $\forall x \in \mathbb{R}$

3. a and f are smooth

Then, there exists a unique and smooth solution to this boundary value problem.

Proof. Consider $-\partial_x \left(a\left(\frac{x}{\varepsilon}\right)\partial_x u_\varepsilon(x)\right) = f$, we have

$$a_\varepsilon(x)\,\partial_x u_\varepsilon(x) = c_\varepsilon - \int_0^x f(x')\,dx'$$

Dividing $a_\varepsilon(x)$ on both sides and by the fundamental theorem of calculus, we have

$$u_\varepsilon(x) - u_\varepsilon(0) = \int_0^x a_\varepsilon^{-1}(x')\left(c_\varepsilon - \int_0^{x'} f(x'')\,dx''\right)dx'$$

By boundary condition $u_\varepsilon(0) = 0$, we have

$$u_\varepsilon(x) = \int_0^x a_\varepsilon^{-1}(x')\left(c_\varepsilon - \int_0^{x'} f(x'')\,dx''\right)dx' \tag{3}$$

To determine the integration constant c_ε, we use boundary conditions $u_\varepsilon(L) = u_\varepsilon(0) = 0$, we have

$$u_\varepsilon(L) - u_\varepsilon(0) = \int_0^L a_\varepsilon^{-1}(x')\left(c_\varepsilon - \int_0^{x'} f(x'')\,dx''\right)dx' = 0$$

$$\Rightarrow c_\varepsilon = \left(\int_0^L a_\varepsilon^{-1}(x')\,dx'\right)^{-1}\int_0^L\int_0^{x'} a_\varepsilon^{-1}(x')\,f(x'')\,dx''dx' \tag{4}$$

Since f and a are smooth, $u_\varepsilon(x)$ is smooth and uniquely determined by c_ε. □

2.1.2 Convergence

Define u_0 to be the unique solution to the equation

$$\begin{cases} -\partial_x(a_0\partial_x u_0) = f & \text{in } O \\ u_0 = 0 & \text{on } \partial O \end{cases} \tag{5}$$

where a_0 denotes the harmonic mean of a, i.e.,

$$a_0 = \frac{1}{\int_0^1 \frac{1}{a(y)}dy}$$

In this section, we prove u_ε converges to u_0 as $\varepsilon \to 0$.
Note that a_0 is constant, so (5) describes a *homogeneous* material with conductivity a_0. By proving the convergence, we have transformed an equation describing a heterogeneous material with a rapidly oscillating conductivity to an equation describing a homogeneous material, which is much simpler to analyze. We, therefore, call (5) the homogenized problem.

Lemma 2.2. *(Convergence of the integral of periodic functions) Let $F(y, x)$ be a smooth function that is periodic in $y \in \mathbb{R}$ with period 1 and assume that F and $\partial_x F$ are bounded. Then,*

$$\lim_{\varepsilon\to 0}\int_a^b F\left(\frac{x}{\varepsilon}, x\right)dx = \int_a^b \bar{F}(x)\,dx, \qquad \bar{F}(x) = \int_0^1 F(y, x)\,dy.$$

Furthermore, show that there exists a constant C (only depending on F) such that

$$\left|\int_a^b F\left(\frac{x}{\varepsilon}, x\right) - \bar{F}(x)\,dx\right| \le C(|b-a|+1)\,\varepsilon$$

Proof. Define function G and $g_\varepsilon(x)$ as:

$$G(y,x) := \int_0^y \left(F(y',x) - \bar{F}(x)\right) dy', \quad g_\varepsilon(x) := \varepsilon G\left(\frac{x}{\varepsilon}, x\right)$$

As F is periodic in y, we have G periodic in y:

$$\begin{aligned} G(y+1,x) - G(y,x) &= \int_y^{y+1} F(y',x) - \bar{F}(x) dy' \\ &= \int_y^{y+1} F(y',x)\, dy' - \int_y^{y+1} \bar{F}(x) dy' \\ &= \int_0^1 F(y',x)\, dy' - \bar{F}(x), \text{ assumed that F is of period 1} \\ &= \bar{F}(x) - \bar{F}(x) = 0 \end{aligned}$$

And $\partial_x G$ is periodic in y:

$$\partial_x G(y+1,x) - \partial_x G(y,x) = \partial_x (G(y+1,x) - G(y,x)) = 0$$

Furthermore, G and $\partial_x G$ are smooth and bounded, and we have

$$\partial_x g_\varepsilon(x) = \varepsilon \partial_x G\left(\frac{x}{\varepsilon}, x\right) + \partial_y G\left(\frac{x}{\varepsilon}, x\right) = \varepsilon \partial_x G\left(\frac{x}{\varepsilon}, x\right) + \left(F\left(\frac{x}{\varepsilon}, x\right) - \bar{F}(x)\right),$$

and thus

$$\begin{aligned} \int_a^b F\left(\frac{x}{\varepsilon}, x\right) - \bar{F}(x) dx &= \int_a^b \partial_x g_\varepsilon(x) - \varepsilon \partial_x G\left(\frac{x}{\varepsilon}, x\right) dx \\ &= \varepsilon\left(G\left(\frac{b}{\varepsilon}, b\right) - G\left(\frac{a}{\varepsilon}, a\right) - \int_a^b \partial_x G\left(\frac{x}{\varepsilon}, x\right) dx\right) \end{aligned}$$

We still need to prove the existence of C:
As G is smooth and differentiable in $[a,b]$, we can apply mean value theorem:

$$\exists\, c \in (a,b), \text{ s.t. } \left|G'\left(\frac{c}{\varepsilon}, c\right)\right| |b-a| = \left|G\left(\frac{b}{\varepsilon}, b\right) - G\left(\frac{a}{\varepsilon}, a\right)\right|$$

Note that by triangular inequality and ML inequality, for any ε we have

$$\begin{aligned} \left|\int_a^b \partial_x G\left(\frac{x}{\varepsilon}, x\right) dx\right| &\leqslant \int_a^b \left|\partial_x G\left(\frac{x}{\varepsilon}, x\right)\right| dx \\ &\leqslant |b-a| \sup_{x\in[a,b]} \left|\partial_x G\left(\frac{x}{\varepsilon}, x\right)\right| \\ &\leqslant |b-a| M, \text{ as } \partial_x G \text{ is bounded } \Rightarrow \exists M \in \mathbb{R} \text{ s.t. } \left|\partial_x G\left(\frac{x}{\varepsilon}, x\right)\right| \leq M, \forall x \end{aligned}$$

and thus

$$\begin{aligned} \left|\int_a^b F\left(\frac{x}{\varepsilon}, x\right) - \bar{F}(x) dx\right| &= \varepsilon \left|G\left(\frac{b}{\varepsilon}, b\right) - G\left(\frac{a}{\varepsilon}, a\right) - \int_a^b \partial_x G\left(\frac{x}{\varepsilon}, x\right) dx\right| \\ &\leq \varepsilon\left(\left|G\left(\frac{b}{\varepsilon}, b\right) - G\left(\frac{a}{\varepsilon}, a\right)\right| + \left|\int_a^b \partial_x G\left(\frac{x}{\varepsilon}, x\right) dx\right|\right) \\ &\leq \varepsilon |b-a| \left[G'\left(\frac{c}{\varepsilon}, c\right) + M\right] \\ &\leq C(|b-a|+1)\varepsilon, \text{ with } C = G'\left(\frac{c}{\varepsilon}, c\right) + M \end{aligned}$$

Clearly, C only depends on F. This finishes the proof. □

Lemma 2.3. *(Convergence of u_ε)* $\max_{x\in O}|u_\varepsilon(x)-u_0(x)|\le C\varepsilon$ *where C only depends on O, f and a.*

Proof. Note that $a_\varepsilon(x)$ has period $\varepsilon \Rightarrow a(1)=a\left(\frac{\varepsilon}{\varepsilon}\right)=a\left(\frac{0}{\varepsilon}\right)=a(0)\Rightarrow a(x)$ has period 1. Write $a_\varepsilon(x)$ as $a_\varepsilon(x)=a\left(\frac{x}{\varepsilon},x\right)$, we can apply Lemma 2.2:

$$\Rightarrow \int_0^L a_\varepsilon^{-1}(x)\,dx=\int_0^L\int_0^1 a^{-1}(y,x)\,dy\,dx+O(\varepsilon)=\int_0^L a_0^{-1}dx+O(\varepsilon)=a_0^{-1}L+O(\varepsilon)$$

where $a_0=\left[\int_0^1 a^{-1}(y,x)\,dy\right]^{-1}$.

To make our later computation easier, first consider arbitrary continuous function F, we have

$$\int_0^x a_\varepsilon^{-1}(x')F(x')\,dx'=\int_0^x\int_0^1 a^{-1}(y,x')\,dyF(x')\,dx'+O(\varepsilon)=a_0^{-1}\int_0^x F(x')\,dx'+O(\varepsilon) \tag{6}$$

Using (6) we have

$$\begin{aligned}
c_\varepsilon &= \left(\int_0^L a_\varepsilon^{-1}(x')\,dx'\right)^{-1}\int_0^L\int_0^{x'} a_\varepsilon^{-1}(x')f(x'')\,dx''dx' \\
&= a_0L^{-1}\int_0^L a_\varepsilon^{-1}(x')\underbrace{\int_0^{x'} f(x'')\,dx''}_{\text{a function of } x'}dx'+O(\varepsilon) \\
&= a_0 \fint_0^L a_0^{-1}\int_0^{x'} f(x'')\,dx''dx'+O(\varepsilon),\ \text{with } \fint_0^L=\frac{1}{L}\int_0^L \\
&= \underbrace{\fint_0^L\int_0^{x'} f(x'')\,dx''dx'}_{c_0}+O(\varepsilon)
\end{aligned}$$

Using (6) again we have

$$\begin{aligned}
u_\varepsilon(x) &= \int_0^x a_\varepsilon^{-1}(x')\underbrace{\left(c_\varepsilon-\int_0^{x'} f(x'')\,dx''\right)}_{\text{a function of } x'}dx' \\
&= \underbrace{a_0^{-1}\int_0^x\left(c_0-\int_0^{x'} f(x'')\,dx''\right)dx'}_{u_0(x)}+O(\varepsilon)
\end{aligned}$$

$\Rightarrow \max_{x\in O}|u_\varepsilon(x)-u_0(x)|\le C\varepsilon$, where C only depends on O, f and a, by the definition of big O notation. Therefore, we showed that $u_\varepsilon(x)$ converges to $u_0(x)$ when $\varepsilon\to 0$. □

Lemma 2.4. *u_0 is smooth and solves* (5).

Proof. As f is smooth, u_0 is smooth. We then need to show u_0 solves (5):

$$-\partial_x(a_0\partial_x u_0)=-\partial_x\left[a_0\cdot a_0^{-1}\left(c_0-\int_0^{x'} f(x'')\,dx''\right)\right]=f$$

□

Lemma 2.5. *Let $f\equiv 1$. Consider the boundary problem:*

$$\begin{cases}-\partial_x(a\partial_x u)=1 & \text{in } O\\ u=0 & \text{on } \partial O\end{cases}$$

The solution to this problem is a quadratic function if and only if the material is homogeneous, i.e., iff a does not depend on x.

Proof. First, we need to find a solution to the boundary value problem :

$$\begin{aligned} -\partial_x (a\partial_x u) &= 1 \\ a\partial_x u &= c - x \\ \partial_x u &= a^{-1}(c-x), c \in \mathbb{R} \text{ is a constant} \\ u(x) &= \int_0^x \frac{c-x'}{a(x')}dx', \text{ as } u(0) = 0 \Rightarrow u'(x) = \frac{c-x}{a(x)} \end{aligned}$$

Hence, $u(x)$ is quadratic $\Leftrightarrow u'(x)$ is affine $\Leftrightarrow a(x)$ constant.
Note that affine function map straight lines to straight lines. Thus, the general equation for affine functions in $1D$ is $y = ax + b$, for some $a,\ b \in \mathbb{R}$. This implies $u(x)$ is quadratic $\Leftrightarrow u'(x)$ is affine. □

Using the homogenization result, certain properties of the heterogeneous equation (2) can be studied by analyzing the homogeneous equation (5):

Lemma 2.6. *Let $f \equiv 1$, $L = 1$. Denote M_ε to be $\max_{\overline{O}} u_\varepsilon$. Then $M_\varepsilon = \frac{1}{8a_0} + O(\varepsilon)$.*

Proof. Denote M_0 to be $\max_{\overline{O}} u_0$.
From Lemma 2.5, we have:

$$\begin{aligned} u_0(x) &= \frac{1}{a_0}\int_0^x c - y\, dy \\ &= \frac{1}{a_0}\left[cy - \frac{1}{2}y^2\right]_0^x \\ &= \frac{1}{a_0}\left(cx - \frac{1}{2}x^2\right) \end{aligned}$$

Using the boundary condition, we have $u_0(1) = 0 \Rightarrow \frac{1}{a_0}(c - \frac{1}{2}) = 0 \Rightarrow c = \frac{1}{2}$
So $u_0(x) = \frac{1}{2a_0}(x - x^2)$
Differentiate, we get $\partial_x u_0(x) = \frac{1}{2a_0}(1 - 2x)$
$\partial_x u_0(x) = 0 \Rightarrow x = \frac{1}{2}$, so $u_0(x)$ achieves its maximum at $x = \frac{1}{2} \Rightarrow M_0 = u_0(\frac{1}{2}) = \frac{1}{8a_0}$
Using Lemma 2.3, we have the following inequalities:

$$\begin{aligned} M_\varepsilon \geq u_\varepsilon(\frac{1}{2}) &= u_0(\frac{1}{2}) + O(\varepsilon) \quad \text{(Lemma 2.3)} \\ &= M_0 + O(\varepsilon) \end{aligned}$$

$$\begin{aligned} \overline{O} \text{ is closed and bounded} &\Rightarrow M_\varepsilon \text{ is attained in } \overline{O} \\ &\Rightarrow \exists x_\varepsilon \in \overline{O} \text{ s.t. } M_\varepsilon = u_\varepsilon(x_\varepsilon) \\ &\Rightarrow M_\varepsilon = u_0(x_\varepsilon) + O(\varepsilon) \quad \text{(Lemma 2.3)} \\ &\Rightarrow M_\varepsilon \leq M_0 + O(\varepsilon) \end{aligned}$$

Combining these two inequalities, we have: $M_\varepsilon = M_0 + O(\varepsilon) = \frac{1}{8a_0} + O(\varepsilon)$ □

We now consider the convergence of $\partial_x u_\varepsilon$.

Lemma 2.7. *Suppose the material is not homogeneous, then* $\limsup \int_O |\partial_x u_\varepsilon - \partial_x u_0|^2 dx > 0$.

Proof. Suppose by contradiction that $\exists$ a sequence (ε_n) $(\lim_{n\to\infty} \varepsilon_n = 0)$ s.t.

$$\lim_{n\to\infty} \sup \int_O |\partial_x u_{\varepsilon_n} - \partial_x u_0|^2 dx = 0$$

This implies that $\partial_x u_{\varepsilon_n}(x) \to \partial_x u_0(x)$ for a.e. $x \in O$ as $n \to \infty$
From Lemma 2.1 we know

$$u_{\varepsilon_n}(x) = \int_0^x a_{\varepsilon_n}^{-1}(x')\left(c_{\varepsilon_n} - \int_0^{x'} f(x'')\, dx''\right) dx' \tag{7}$$

From Lemma 2.3 we know

$$u_0(x) = a_0^{-1}\int_0^x \left(c_0 - \int_0^{x'} f(x'')\,dx''\right)dx' \tag{8}$$

Differentiate, we get

$$\partial_x u_{\varepsilon_n}(x) = \frac{1}{a_{\varepsilon_n}(x)}\left(c_{\varepsilon_n} - \int_0^x f(x')\,dx'\right)$$

$$\partial_x u_0(x) = \frac{1}{a_0}\left(c_0 - \int_0^x f(x')\,dx'\right)$$

From Lemma 2.3, we know $c_{\varepsilon_n} = c_0 + O(\varepsilon_n) \Rightarrow c_{\varepsilon_n} \to c_0$ as $n \to \infty$
So we have $a_{\varepsilon_n}(x) \to a_0$ for a.e. $x \in O$ as $n \to \infty$
Using the dominated convergence theorem, we have

$$\int_O a_{\varepsilon_n}(x)\,dx \to \int_O a_0\,dx$$

However, by Lemma 2.2,

$$\begin{aligned}\int_O a_{\varepsilon_n}(x)\,dx &= \int_O a(\frac{x}{\varepsilon_n}, x)\,dx \\ &\to \int_O \int_0^1 a(y,x)\,dydx\end{aligned}$$

So it must be the case that

$$a_0 = \int_0^1 a(y)dy$$

$$\Rightarrow \int_0^1 \frac{1}{a(y)}\,dy = \frac{1}{\int_0^1 a(y)\,dy}$$

which is only true when $a(x)$ is constant, i.e., independent of x. Contradiction. ◻

Lemma 2.8. *$\forall$ smooth functions $\varphi : \mathbb{R} \to \mathbb{R}$ we have:*

$$\int_O u_\varepsilon'(x)\varphi(x)\,dx \to \int_O u_0'(x)\varphi(x)\,dx$$

Proof.

$$\begin{aligned}I &= \int_O [u_\varepsilon'(x) - u_0'(x)]\varphi(x)\,dx \\ &= [(u_\varepsilon(x) - u_0(x))\varphi(x)]_{\partial O} - \int_O [u_\varepsilon(x) - u_0(x)]\varphi'(x)\,dx \quad \text{(integration by parts)} \\ &= -\int_O [u_\varepsilon(x) - u_0(x)]\varphi'(x)\,dx \quad (u_\varepsilon = u_0 = 0 \text{ on } \partial O)\end{aligned}$$

From Lemma 2.3, $\max_{x\in O} |u_\varepsilon(x) - u_0(x)| \le C\varepsilon$.

$$\begin{aligned}|I| &\le L\left(\sup_{x\in O}|u_\varepsilon(x) - u_0(x)||\varphi'(x)|\right) \\ &\le C\varepsilon\left(L\sup_{x\in O}|\varphi'(x)|\right)\end{aligned}$$

Since φ is defined on $\mathbb{R}$ and smooth, O is bounded, $\sup_{x\in O}|\varphi'(x)|$ is finite.
So we have

$$\begin{aligned}
&|I| \to 0 \text{ as } \varepsilon \to 0\\
\Rightarrow\quad &I \to 0 \text{ as } \varepsilon \to 0\\
\Rightarrow &\int_O u_\varepsilon'(x)\varphi(x)\,dx \to \int_O u_0'(x)\varphi(x)\,dx \text{ as } \varepsilon \to 0
\end{aligned}$$

□

Lemma 2.7 and 2.8 show that for $\partial_x u_\varepsilon$, we have weak convergence, but not strong convergence. Lemma 2.9 will show that by modifying u_0 by adding oscillations, we achieve strong convergence.

Lemma 2.9. *(Two-scale expansion) Let a, f be as above (defined in (2)), $L = 1$, (i.e., $O = (0, 1)$). Let $\phi : \mathbb{R} \to \mathbb{R}$ denote a 1-periodic solution to*

$$\partial_y \left(a(y)\left(\partial_y\phi(y) + 1\right)\right) = 0 \tag{9}$$

with $\phi(0) = 0$. Let u_0 and u_ε be defined as above. Consider

$$v_\varepsilon(x) := u_0(x) + \varepsilon\,\phi(\frac{x}{\varepsilon})\,\partial_x u_0(x)$$

Then $\exists$ a constant $C > 0$ s.t. $\forall\varepsilon > 0$ with $\frac{1}{\varepsilon} \in \mathbb{N}$ we have

$$\int_O |u_\varepsilon - v_\varepsilon|^2 + |\partial_x u_\varepsilon - \partial_x v_\varepsilon|^2 \le \frac{4}{\lambda^2}\max|\phi|^2\varepsilon^2\int_O |\partial_x^2 u_0|^2$$

Proof. Step 1. Find $\phi(y)$
Solve (9) for ϕ:

$$\begin{aligned}
&\partial_y(a(y)(\partial_y\phi(y) + 1)) = 0\\
&a(y)(\partial_y\phi(y) + 1) = c,\ c \text{ is a constant in } \mathbb{R}\\
&\Rightarrow \phi(y) = \int_0^y \frac{c}{a(t)} - 1dt,\ \text{ as } \phi(0) = 0
\end{aligned}$$

Determine c:
Since ϕ is 1-periodic, a is of period 1 and $\phi(0) = 0$, we have $\phi(1) = 0$.

$$\begin{aligned}
&\Rightarrow \phi(1) = \int_0^1 \frac{c}{a(t)} - 1\,dt\\
&\Rightarrow 0 = \int_0^1 \frac{c}{a(t)}dt - 1\\
&\Rightarrow c\int_0^1 \frac{1}{a(t)}dt = 1\\
&\Rightarrow c = \frac{1}{\int_0^1 \frac{1}{a(t)}\,dt} = a_0
\end{aligned}$$

Therefore,

$$\phi(y) = \int_0^y \frac{a_0}{a(t)} - 1\,dt \text{ with } a_0 = a(y)(\partial_y\phi(y) + 1)$$

By assumption a is smooth, so ϕ is smooth. Given ϕ is also periodic, we conclude ϕ is bounded.

Step 2: We consider $z_\varepsilon = u_\varepsilon - v_\varepsilon$. From the assumption, we have a is 1-periodic, thus we have

$$\begin{aligned}
\phi(y) &= \int_0^y \frac{a_0}{a(t)} - 1\, dt \\
&= a_0 \int_0^y \frac{1}{a(t)} dt - \int_0^y 1 dt \\
&= a_0 \cdot y \int_0^1 \frac{1}{a(t)} dt - y, \text{ if } y \in \mathbb{N} \text{ as } a \text{ is of period 1} \\
&= 0, \text{ by definition of } a_0 \\
\Rightarrow \phi\left(\frac{1}{\varepsilon}\right) &= 0, \text{for } \frac{1}{\varepsilon} \in \mathbb{N}
\end{aligned}$$

By the boundary conditions of u_ε and ϕ_ε, we have $z_\varepsilon(0) = z_\varepsilon(1) = 0$.

Claim:

$$\int_O |z_\varepsilon|^2 \leq \int_O |\partial_x z_\varepsilon|^2$$

Proof of claim: By Poincaré's inequality $\left(\forall u \in H_0^1(0,1), \int_0^1 u^2 dx \leqslant \int_0^1 (u')^2\, dx\right)$[7], we have

$$\int_0^1 |z_\varepsilon|^2 = \int_0^1 \left(\int_0^x \partial_x z_\varepsilon\right)^2 \leqslant \int_0^1 \left|\partial_x \left(\int_0^x \partial_x z_\varepsilon\right)\right|^2 = \int_0^1 |\partial_x z_\varepsilon|^2$$

$\Rightarrow \int_O |z_\varepsilon|^2 + |\partial_x z_\varepsilon|^2 \leqslant 2 \int_O |\partial_x z_\varepsilon|^2 \leqslant \frac{2}{\lambda} \int_O |\partial_x z_\varepsilon|^2\, a_\varepsilon$, by the assumption that a is uniformly elliptic $\Rightarrow \exists \lambda$ s.t. $\lambda \leqslant a_\varepsilon$

Integrating by parts, we have

$$\begin{aligned}
&\int_O a_\varepsilon\, |\partial_x z_\varepsilon|^2 \\
&= \int_O a_\varepsilon \partial_x z_\varepsilon \partial_x z_\varepsilon \\
&= z_\varepsilon \cdot a_\varepsilon \partial_x z_\varepsilon|_{\partial O} - \int_O z_\varepsilon \partial_x \left(a_\varepsilon \partial_x z_\varepsilon\right) \\
&= \int_O z_\varepsilon \left[-\partial_x \left(a_\varepsilon \partial_x z_\varepsilon\right)\right], \text{ as } z_\varepsilon = 0 \text{ on } \partial O \\
\Rightarrow &\int_O |z_\varepsilon|^2 + |\partial_x z_\varepsilon|^2 \leqslant \frac{2}{\lambda} \int_O z_\varepsilon \left[-\partial_x \left(a_\varepsilon \partial_x z_\varepsilon\right)\right]
\end{aligned}$$

Step 3. Compute $-\partial_x \left(a_\varepsilon \partial_x z_\varepsilon\right)$

$$\begin{aligned}
\partial_x z_\varepsilon &= \partial_x \left(u_\varepsilon - u_0 - \varepsilon \phi_\varepsilon \partial_x u_0\right) \\
&= \partial_x u_\varepsilon - \partial_x u_0 - \varepsilon \partial_x \phi_\varepsilon \partial_x u_0 - \varepsilon \phi_\varepsilon \partial_x^2 u_0 \\
&= \partial_x u_\varepsilon - \left(\partial_y \phi\left(\frac{x}{\varepsilon}\right) + 1\right) \partial_x u_0 - \varepsilon \phi_\varepsilon \partial_x^2 u_0, \text{ as } \varepsilon \partial_x = \partial_y \text{ with } y = \frac{x}{\varepsilon}
\end{aligned}$$

By $a_0 = a_\varepsilon \left(\partial_y \phi(\frac{\cdot}{\varepsilon}) + 1\right)$, we have

$$\begin{aligned}
a_\varepsilon \partial_x z_\varepsilon &= a_\varepsilon \partial_x u_\varepsilon - a_0 \partial_x u_0 - a_\varepsilon \varepsilon \phi_\varepsilon \partial_x^2 u_0 \\
\Rightarrow -\partial_x \left(a_\varepsilon \partial_x z_\varepsilon\right) &= -\partial_x \left(a_\varepsilon \partial_x u_\varepsilon\right) + \partial_x \left(a_0 \partial_x u_0\right) + \partial_x \left(\varepsilon a_\varepsilon \phi_\varepsilon \partial_x^2 u_0\right)
\end{aligned}$$

Note $-\partial_x \left(a_\varepsilon \partial_x u_\varepsilon\right) = -\partial_x \left(a_0 \partial_x u_0\right) = f$, according to equation (2) and (5), so the equation is simplified to

$$-\partial_x \left(a_\varepsilon \partial_x z_\varepsilon\right) = \partial_x \left(\varepsilon a_\varepsilon \phi_\varepsilon \partial_x^2 u_0\right)$$

Combined with the result of Step 2, we have

$$
\begin{aligned}
\int_O |z_\varepsilon|^2 + |\partial_x z_\varepsilon|^2 &\leqslant \frac{2}{\lambda}\int_O z_\varepsilon\left[-\partial_x\left(a_\varepsilon \partial_x z_\varepsilon\right)\right] \\
&= \frac{2}{\lambda}\int_O z_\varepsilon\left[\partial_x\left(\varepsilon a_\varepsilon \phi_\varepsilon \partial_x^2 u_0\right)\right] \\
&= \frac{2}{\lambda}\left([z_\varepsilon \varepsilon a_\varepsilon \phi_\varepsilon \partial_x^2 u_0]_{\partial O} - \int_O \partial_x z_\varepsilon \varepsilon a_\varepsilon \phi_\varepsilon \partial_x^2 u_0\right) \quad \text{(integration by parts)} \\
&= -\frac{2}{\lambda}\int_O \partial_x z_\varepsilon \varepsilon a_\varepsilon \phi_\varepsilon \partial_x^2 u_0, \quad \text{as } z_\varepsilon = 0 \text{ on } \partial O \\
&\leq \frac{2}{\lambda}\sqrt{\int_O (\partial_x z_\varepsilon)^2}\sqrt{\int_O (\varepsilon a_\varepsilon \phi_\varepsilon \partial_x^2 u_0)^2} \quad \text{(Cauchy-Schwarz)} \\
&\leq \frac{2}{\lambda}\left[\frac{\lambda}{4}\int_O (\partial_x z_\varepsilon)^2 + \frac{1}{\lambda}\int_O (\varepsilon a_\varepsilon \phi_\varepsilon \partial_x^2 u_0)^2\right] \\
&\qquad \text{(Young's inequality in the form } ab \leq \frac{\delta}{2}a^2 + \frac{1}{2\delta}b^2\text{, with } \delta = \frac{\lambda}{2}) \\
&= \frac{1}{2}\int_O |\partial_x z_\varepsilon|^2 + \frac{2}{\lambda^2}\varepsilon^2 \int_O |a_\varepsilon|^2 |\phi_\varepsilon|^2 |\partial_x^2 u_0|^2
\end{aligned}
$$

$$
\begin{aligned}
&\Rightarrow \int_O |z_\varepsilon|^2 + \frac{1}{2}|\partial_x z_\varepsilon|^2 \leq \frac{2}{\lambda^2}\varepsilon^2 \int_O |a_\varepsilon|^2 |\phi_\varepsilon|^2 |\partial_x^2 u_0|^2 \\
&\Rightarrow \int_O |z_\varepsilon|^2 + |\partial_x z_\varepsilon|^2 \\
&\leq 2\left(\int_O |z_\varepsilon|^2 + \frac{1}{2}|\partial_x z_\varepsilon|^2\right) \\
&\leq \frac{4}{\lambda^2}\varepsilon^2 \int_O |a_\varepsilon|^2 |\phi_\varepsilon|^2 |\partial_x^2 u_0|^2 \\
&\leq \frac{4}{\lambda^2}\varepsilon^2 \int_O |\phi_\varepsilon|^2 |\partial_x^2 u_0|^2 \quad (a \text{ is uniformly elliptic by assumption, so } a(x) \leq 1 \forall x \in \mathbb{R}) \\
&\leq \frac{4}{\lambda^2}\max|\phi|^2 \varepsilon^2 \int_O |\partial_x^2 u_0|^2 \quad (\phi \text{ is bounded})
\end{aligned}
$$

□

2.2 Stochastic

A similar result is also achieved in the stochastic case. However, the setting of the problem is rather different from what we have seen in Year 2 syllabus and this section is introduced in a heuristic way, by providing some main results of homogenization and some intuitions behind it. The main results of this section are from Alen Alexanderian's notes[1] and Josselin Garnier's article[3].

We are interested in the solution u_ε of the equation

$$
\begin{cases} -\partial_x\left(a\left(\frac{x}{\varepsilon},\omega\right)\partial_x u_\varepsilon(x)\right) = f & 0 < x < 1, \omega \in \Omega \\ u_\varepsilon(x,\omega) = 0 & x = 0, 1 \end{cases} \tag{10}
$$

Here $a(x,\omega) : (0,1)\times\Omega \to \mathbb{R}$, where $(\Omega, \mathcal{F}, \mathbb{P})$ is an abstract probability space, satisfies three conditions:

- Bounded
  $\exists\, \alpha, \beta > 0$ s.t. $\alpha \leq a \leq \beta$ a.e. for $(x,\omega) \in (0,1)\times\Omega$
- Stationary
  $\forall x, y \in (0,1)$, $a(x,\cdot) \overset{\mathcal{L}}{=} a(y,\cdot)$ (i.e., they have the same distribution)

- Ergodic
  Let $A \subset \mathbb{R}$ be bounded, then $\forall F : \mathbb{R} \to \mathbb{R}$, s.t. F bounded and continuous, we have

  (1)
$$\fint_A F(a(Rx, \omega))dx \xrightarrow{\text{a.s.}} \mathbb{E}\left[F(a(0, \omega))\right] \quad \text{as } R \to \infty$$

  (2) $\forall g : A \to \mathbb{R}$, s.t. g is smooth and has a compact support, we have
$$\fint_A F(a(Rx, \omega))g(x)dx \xrightarrow{\text{a.s.}} \mathbb{E}\left[F(a(0, \omega))\right] \fint_A g(x)dx \quad \text{as } R \to \infty$$

  Note that using change of variable $\varepsilon = \frac{1}{R}$, we get

  (1*)
$$\fint_A F(a(\frac{x}{\varepsilon}, \omega))dx \xrightarrow{\text{a.s.}} \mathbb{E}\left[F(a(0, \omega))\right] \quad \text{as } \varepsilon \to 0$$

  (2*)
$$\fint_A F(a(\frac{x}{\varepsilon}, \omega))g(x)dx \xrightarrow{\text{a.s.}} \mathbb{E}\left[F(a(0, \omega))\right] \fint_A g(x)dx \quad \text{as } \varepsilon \to 0$$

Our goal is to prove that under these conditions, u_ε converges almost surely to $\bar{u}$, which is the solution of the equation
$$\begin{cases} -\partial_x\left(\bar{a}\partial_x\bar{u}\,(x)\right) = f & 0 < x < 1 \\ \bar{u}(x) = 0 & x = 0, 1 \end{cases} \tag{11}$$
where
$$\bar{a} = \frac{1}{\mathbb{E}[\frac{1}{a(0,\omega)}]}$$

Lemma 2.10. *(Convergence almost surely)* $\forall x \in (0, 1) : \ u_\varepsilon(x, \omega) \xrightarrow{a.s.} \bar{u}(x) \quad \textit{as } \varepsilon \to 0$

Proof. Recall from Lemma 2.1, the solution $u_\varepsilon(x, \omega)$ can be expressed as:
$$\begin{aligned} \forall \omega \in \Omega : \ u_\varepsilon\,(x, \omega) &= \int_0^x a_\varepsilon^{-1}\,(y, \omega)\left(c_\varepsilon(\omega) - \int_0^y f\,(z)\,dz\right)dy \\ &= c_\varepsilon(\omega)\int_0^x \frac{1}{a_\varepsilon(y, \omega)}dy - \int_0^x \frac{\int_0^y f(z)dz}{a_\varepsilon(y, \omega)}dy \\ \text{where } c_\varepsilon(\omega) &= \left(\int_0^1 a_\varepsilon^{-1}\,(y, \omega)\,dy\right)^{-1}\int_0^1\int_0^y a_\varepsilon^{-1}\,(y, \omega)\,f\,(z)\,dzdy \end{aligned}$$
Solving (11), we have
$$\bar{u}(x) = \bar{c}\frac{x}{\bar{a}} - \frac{1}{\bar{a}}\int_0^x\int_0^y f(z)\,dzdy$$
where
$$\bar{c} = \int_0^1\int_0^y f(z)\,dzdy$$
We consider the two quantities in the expression u_ε.
Step 1. First consider
$$\int_0^x \frac{\int_0^y f(z)dz}{a_\varepsilon(y, \omega)}dy = \int_0^x \frac{\int_0^y f(z)dz}{a(\frac{y}{\varepsilon}, \omega)}dy$$

Using (2*), with $F : x \to \frac{1}{x},\ g : x \to \int_0^x f(y)\,dy,\ A = (0, x)$
We have

$$\frac{1}{x}\int_0^x \frac{\int_0^y f(z)dz}{a(\frac{y}{\varepsilon},\omega)}dy \xrightarrow{\text{a.s.}} \mathbb{E}\left[\frac{1}{a(0,\omega)}\right]\frac{1}{x}\int_0^x\int_0^y f(z)\,dzdy \quad \text{as } \varepsilon \to 0$$

$$\Rightarrow \int_0^x \frac{\int_0^y f(z)dz}{a(\frac{y}{\varepsilon},\omega)}dy \xrightarrow{\text{a.s.}} \mathbb{E}\left[\frac{1}{a(0,\omega)}\right]\int_0^x\int_0^y f(z)\,dzdy \quad \text{as } \varepsilon \to 0$$

Step 2. Now we consider

$$c_\varepsilon(\omega)\int_0^x \frac{1}{a_\varepsilon(y,\omega)}dy$$

Using (1*), with $F : x \to \frac{1}{x},\ A = (0, 1)$
We have

$$\int_0^1 \frac{1}{a_\varepsilon(y,\omega)}dy = \int_0^1 \frac{1}{a(\frac{y}{\varepsilon},\omega)}dy \xrightarrow{\text{a.s.}} \mathbb{E}\left[\frac{1}{a(0,\omega)}\right] \quad \text{as } \varepsilon \to 0$$

Similar to Step 1, using (2*), with everything else kept the same except $A = (0, 1)$, we have

$$\int_0^1 \frac{\int_0^y f(z)dz}{a(\frac{y}{\varepsilon},\omega)}dy \xrightarrow{\text{a.s.}} \mathbb{E}\left[\frac{1}{a(0,\omega)}\right]\int_0^1\int_0^y f(z)\,dzdy \quad \text{as } \varepsilon \to 0$$

Combining these, we have

$$c_\varepsilon(\omega) \xrightarrow{\text{a.s.}} \int_0^1\int_0^y f(z)\,dzdy \quad \text{as } \varepsilon \to 0$$

In other words,

$$c_\varepsilon(\omega) \xrightarrow{\text{a.s.}} \bar{c} \quad \text{as } \varepsilon \to 0$$

Using (1*) again with $A = (0, x)$, we have

$$\frac{1}{x}\int_0^x \frac{1}{a_\varepsilon(y,\omega)}dy \xrightarrow{\text{a.s.}} \mathbb{E}\left[\frac{1}{a(0,\omega)}\right] \quad \text{as } \varepsilon \to 0$$

Therefore

$$c_\varepsilon(\omega)\int_0^x \frac{1}{a_\varepsilon(y,\omega)}dy \xrightarrow{\text{a.s.}} \bar{c}\,x\,\mathbb{E}\left[\frac{1}{a(0,\omega)}\right] \quad \text{as } \varepsilon \to 0$$

In conclusion, we have

$$\begin{aligned}
& u_\varepsilon(x,\omega) \xrightarrow{\text{a.s.}} \bar{c}\,x\,\mathbb{E}\left[\frac{1}{a(0,\omega)}\right] - \mathbb{E}\left[\frac{1}{a(0,\omega)}\right]\int_0^x\int_0^y f(z)\,dzdy \quad \text{as } \varepsilon \to 0 \\
\Rightarrow \quad & u_\varepsilon(x,\omega) \xrightarrow{\text{a.s.}} \bar{c}\,\frac{x}{\bar{a}} - \frac{1}{\bar{a}}\int_0^x\int_0^y f(z)\,dzdy \quad \text{as } \varepsilon \to 0 \\
\Rightarrow \quad & u_\varepsilon(x,\omega) \xrightarrow{\text{a.s.}} \bar{u}(x) \quad \text{as } \varepsilon \to 0
\end{aligned}$$

□

One can also show a similar weak-convergence result for $\partial_x u_\varepsilon(x,\omega)$. Recall from Lemma 2.1 that $\partial_x u_\varepsilon(x,\omega)$ and $\partial_x \bar{u}(x)$ can be written as:

$$\partial_x u_\varepsilon(x,\omega) = \frac{1}{a_\varepsilon(x,\omega)}\left(c_\varepsilon(\omega) - \int_0^x f(y)dy\right)$$

$$\partial_x \bar{u}(x) = \frac{1}{\bar{a}}\left(\bar{c} - \int_0^x f(y)dy\right)$$

Using a similar techniques as presented in Lemma 2.8, one can show:

$$\forall \text{smooth function } \phi : \mathbb{R} \to \mathbb{R}, \int_0^1 u'_\varepsilon(x)\phi(x)\,dx \xrightarrow{\text{a.s.}} \int_0^1 \bar{u}(x)\phi(x)\,dx \text{ as } \varepsilon \to 0$$

By Lemma 2.10 and the fact that $\underset{x\in[0,1]}{sup}\,|u_\varepsilon(x,\omega)| \leq C$, where C is independent from ε (follow from explicit representation from u_ε). Then by the dominated convergence theorem, the result above follows.
One can also show a two-scale expansion result by considering the corrector problem in 1-D:

$$\forall \omega \in \Omega : \partial_y(a(y,\omega)(\partial_y\phi(y,\omega)+1)) = 0 \,; \phi(0,\omega) = 0$$

One can also get a representation that, as in Lemma 2.9:

$$\phi(y,\omega) = \int_0^y \frac{\bar{a}}{a(x,\omega)} - 1\,dx$$

From one of the results from Stefan Neukamm's lecture notes [8], we obtain that $\phi(x)$ is not too large as $x \to \infty$, with an asymptotic result:

$$\forall \omega \in \Omega : \phi(x,\omega) \sim O(x^\alpha),\ \alpha < 1$$

Analogous to the two scale expansion results, we know that the corrected-solution can be written as:

$$v_\varepsilon(x) = \bar{u}(x) + \varepsilon\phi\left(\frac{x}{\varepsilon}\right)\partial_x\bar{u}(x)$$

Thus, by replacing the term $\underset{x\in\mathbb{R}}{max}\,\phi(x)$, we can obtain an analogous result as in Lemma 2.9:

$$\int_O |u_\varepsilon - v_\varepsilon|^2 + |\partial_x u_\varepsilon - \partial_x v_\varepsilon|^2 \xrightarrow{\text{a.s.}} 0$$

The theory of homogenization in 1D depends highly on the fact that we have an explicit representation for the solution. But in higher dimensions, such regular behaviour may not be obtained which makes the theory more involved. In the next section, we will develop homogenization theories for multi-dimensional PDEs with periodic coefficients.

3 Theories in Multi-Dimensions for Periodic Homogenization

In this section, we will develop how to homogenize the multidimensional PDE with the periodic elliptical operator. Here, instead of proving everything from scratch, we are giving a more intuitive way of deriving the homogenized problem and seeing the actual convergence. Main ideas come from [6],[8] and [9].

3.1 Setting of the Problem

Similar to 1D homogenization, we wish to homogenize the elliptic operator $-\nabla \cdot (a\nabla)$ under periodic domain Ω (a bounded open set in $\mathbb{R}^N$). Domain Ω has period ε(a positive number in microscale (very small)) and the corresponding cell Y. The diffusion coefficient a is a multi-dimensional tensor in Ω given by a $N \times N$ matrix $A(x, \frac{x}{\varepsilon})$ where $A(x, y)$ is a Y-periodic function of fast variable $y \in Y$.
Furthermore, matrix A satisfies the usual coerciveness and boundedness assumptions: $\exists$ positive constant α and β with $0 < \alpha \leq \beta$ such that for any constant vector $\xi \in \mathbb{R}^N$ and at any point $(x, y) \in \Omega \times Y$,

$$\alpha|\xi|^2 \leq \sum_{i,j=1}^{N} A_{i,j}(x, y)\xi_i\xi_j \leq \beta|\xi|^2, \tag{12}$$

where $A_{i,j}$ denotes the entries of A.
Denoting the source term by $f(x)$ then our boundary value problem becomes:

$$\begin{cases} -\nabla \cdot (A(x, \frac{x}{\varepsilon})\nabla u_\varepsilon) = f & in\ \Omega, \\ u_\varepsilon = 0 & on\ \partial\Omega. \end{cases} \tag{13}$$

To simplify our notation, we used $A_\varepsilon(x)$ to denote $A(x, \frac{x}{\varepsilon})$.

3.2 Existence and Uniqueness of the Weak Solution

Under the condition on our boundary value problem, we seek Lax-Milgram Lemma to give existence and uniqueness of the solution. The new concept comes from the notes by Christophe Prange [9].

Lemma 3.1. *The equation (13) admits a unique weak solution u_ε in the space $H_0^1(\Omega)$. Moreover, u_ε satisfies the priori estimate:*

$$||u_\varepsilon||_{H_0^1(\Omega)} \leq C||f||_{L^2(\Omega)}$$

where C is a positive constant independent of ε.

Proof. For any test function ϕ on Ω with $\phi|_{\partial\Omega} = 0$, the weak solution is:

$$\int_\Omega \nabla \cdot (A_\varepsilon(x)\nabla u_\varepsilon(x)) \cdot \phi + \int_\Omega f\phi = 0$$

Using Green's first identity for the first integral, we have:

$$\int_\Omega \nabla \cdot (A_\varepsilon(x)\nabla u_\varepsilon(x)) \cdot \phi = \int_{\partial\Omega} \phi A_\varepsilon(x)\nabla u_\varepsilon(x) - \int_\Omega \nabla\phi \cdot A_\varepsilon \nabla u_\varepsilon(x)$$

The first integral is 0 as $\phi|_{\partial\Omega} = 0$, hence:

$$\int_\Omega A_\varepsilon(x)\nabla u_\varepsilon(x) \cdot \nabla\phi(x)dx = \int_\Omega f(x)\phi(x)dx \tag{14}$$

By Lax-Milgram Theorem, this weak formulation will give a unique weak solution satisfying equation (14).
Taking $\phi = u_\varepsilon$ in the weak solution, using Poincaré inequality, the priori bound is:

$$||\nabla u_\varepsilon||_{L^2(\Omega)} \leq D||f||_L^2(\Omega)$$

for a positive constant number D.
Therefore, using Poincaré inequality one more time, u_ε is bounded.

$$||u_\varepsilon||_{H_0^1(\Omega)} \leq C||f||_{L^2(\Omega)}$$

for some positive constant C. □

This allows us to give further derivation.

3.3 The Two-scale Asymptotic Expansions: Derivation of Homogenized Coefficients

To derive the homogenized problem, we will start from separating the macroscopic scale, from the microscopic scale(scale ε). For simplicity, from now on, we will assume that our diffusion coefficient A is differentiable. Now, the main idea and assumption comes from [6] where we formally assume the unknown function u_ε has an asymptotic expansion of the form:

$$u_\varepsilon(x) = u_0(x,y) + \varepsilon u_1(x,y) + \varepsilon^2 u_2(x,y) + ..., \tag{15}$$

where the functions u_i are periodic in the "fast" variable $y = \frac{x}{\varepsilon}$.
So the derivatives obey the law,

$$\nabla = \nabla_x + \frac{1}{\varepsilon}\nabla_y$$

where the subscripts denote the partial derivatives with respect to x and y respectively. Using this expansion, we evaluate the equation to find that

$$-(\nabla_x + \frac{1}{\varepsilon}\nabla_y) \cdot [A(y)(\frac{1}{\varepsilon}\nabla_y u_0 + \nabla_x u_0 + \nabla_y u_1 + \varepsilon\nabla_x u_1 + \varepsilon^2\nabla_x u_2 + \varepsilon\nabla_y u_2 + ...)] = f$$

We evaluate each term in ascending power of ε. We get the formula:

$$\begin{aligned}
&\varepsilon^{-2}\nabla_y \cdot (A(y)\nabla_y u_0(x,y))+\\
&\varepsilon^{-1}(\nabla_y \cdot (A(y)\nabla_x u_0(x,y)) + \nabla_y \cdot (A(y)\nabla_y u_1(x,y)) + A(y)\nabla_x \cdot \nabla_y u_0(x,y))+\\
&\varepsilon^{0}(\nabla_y \cdot (A(y)\nabla_y u_2(x,y)) + \nabla_y \cdot (A(y)\nabla_x u_1(x,y)) + A(y)\nabla_x \cdot \nabla_y u_1(x,y) + A(y)\nabla_x \cdot \nabla_x u_0(x,y))+\\
&... + f(x) = 0
\end{aligned} \tag{16}$$

Considering the coefficients of the different ε powers in this equation.
The equation of term ε^{-2} gives:

$$\nabla_y \cdot (A(y)\nabla_y u_0(x,y)) = 0 \text{ for } y \in Y$$

Because $u_0(x,y)$ is Y-periodic in the variable y, $u_0(x,y) = u_0(x)$ is a function of x alone, which is independent of y. This means: for the ε^{-1} term:

$$A(y)\nabla_x \cdot \nabla_y u_0(x) = 0$$

and hence:

$$\nabla_y \cdot (A(y)\nabla_y u_1(x,y)) = -\nabla_y \cdot (A(y)\nabla_x u_0(x)) \text{ for } y \in Y \tag{17}$$

At this point, we wish to express the function $u_1(x,y)$ in terms of function $u_0(x,y)$.
First, noticed that:

$$\nabla_x u_0(x) = \Sigma_{j=1}^{N}\vec{e_j}\partial_{x_j}u_0(x) \tag{18}$$

Therefore, we can simplify our expression:

$$\nabla_y \cdot (A(y)\nabla_y u_1(x,y)) = -\sum_{j=1}^{N}\partial_{y_j}A(y)\partial_{x_j}u_0(x) \text{ for } y \in Y$$

Define the differential operator on variable y as $L_y := \nabla_y \cdot (A(y)\nabla_y)$:
Our equation (17) is now:

$$L_y[u_1(x,y)] = -\sum_{j=1}^{N}\partial_{y_j}A(y) \cdot \partial_{x_j}u_0(x)$$

Notice that the first term $-\partial_{y_j}A(y)$ is purely a function of y, and the second term $\partial_{x_j}u_0(x)$ is purely a function of x, say $\lambda(x) = \sum_{j=1}^{N}\partial_{x_j}u_0(x)$.Then we have:

if w(y) is the function such that component-wise $L_y[w_i] = -\partial_{y_i} A(y)\vec{e_i}$, then: $\lambda(x)w(y)$ solves the equation (17),

$$\text{i.e.} u_1(x,y) = \lambda(x)w(y) = \sum_{j=1}^{N} w_j(y)\partial_{x_j} u_0(x)$$

Here, for each $j = 1, 2, ..., N$, we can very naturally define the so-called cell-problem or the corrector equation, as the functions w_j(homogenization correctors) are defined as the Y-periodic solution of it:

$$\nabla_y \cdot (A(y)\nabla_y w_j(y)) = -\nabla_y \cdot (A(y)\vec{e_j}) \; for \; y \in Y$$

Differentiating the term for $u_1(x,y)$, we immediately get the expression which can simplify our equation a lot later:

$$\nabla_y u_1(x,y) = \sum_{j=1}^{N} \nabla_y w_j(y)\partial_{x_j} u_0(x) \tag{19}$$

We then go further in our equation (16) for the term ε^0.We get

$$\nabla_y \cdot [A(y)\nabla_y u_2(x,y)] + \nabla_y \cdot [A(y)\nabla_x u_1(x,y)] + A(y)\nabla_x \cdot \nabla_y u_1(x,y) + A(y)\nabla_x \cdot \nabla_x u_0(x) + f(x) = 0 \; for \; y \in Y$$

We integrate this identity over the cell Y and obtain:

$$-\fint_Y \nabla_y \cdot [A(y)\nabla_y u_2(x,y)]dy = \fint_Y \Big(\nabla_y \cdot (A(y)\nabla_x u_1(x,y)) + A(y)\nabla_x \cdot \nabla_y u_1(x,y) + A(y)\nabla_x^2 u_0(x) + f(x)\Big)\, dy \tag{20}$$

For this equation, we are having an expression for $u_2(x,y)$. As $u_2(x,y)$ is defined to be periodic in Y, the integral on the left hand side will need to be 0 in order to have a solution. Hence, we get the following:

$$\fint_Y \Big(\nabla_y \cdot (A(y)\nabla_x u_1(x,y)) + A(y)\nabla_x \cdot \nabla_y u_1(x,y) + A(y)\nabla_x^2 u_0(x) + f(x)\Big)\, dy = 0 \tag{21}$$

Then we separately deal with the integral, for the first integral, using Green's first identity and get:

$$\fint_Y \nabla_y \cdot (A(y)\nabla_x u_1(x,y))dy = \int_{\partial Y} \vec{v} \cdot (A(y)\nabla_x u_1(x,y))d\Gamma(y) = 0$$

where $\vec{v}$ is the normal vector on ∂Y.
This boundary integral vanishes because of the Y-periodicity of the functions $u_1(x,y)$.
Hence we have the following integral equation:

$$\fint_Y A(y)\nabla_x \cdot \nabla_y u_1(x,y)dy + \fint_Y A(y)dy\nabla_x^2 u_0(x) + \fint_Y f(x)dy = 0 \tag{22}$$

We use the expression (18) and (19) and use the Einstein's summation convention:

$$\begin{aligned} &A(y)\nabla_x \cdot \nabla_y u_1(x,y) + A(y)\nabla_x \cdot \nabla_x u_0(x) \\ &= A(y)\nabla_x \cdot (\nabla_y w_i(y)\partial_{x_j} u_0 + \partial_{x_i} u_0 \vec{e_i}) \\ &= \nabla_x \cdot [A(y)(\nabla_y w_i(y) + \vec{e_i})\partial_{x_i} u_0(x)] \end{aligned}$$

Substitute it back to equation (22), we have the following:

$$\fint_Y \nabla_x \cdot [A(y)(\nabla_y w_i(y) + \vec{e_i})\partial_{x_i} u_0(x)] + \fint_Y f(x)dy = 0 \tag{23}$$

As the integral is 0 for this equation, f is arbitrary function, we need:

$$-\nabla_x \cdot [A(y)(\vec{e_i} + \nabla w_i(y))\partial_{x_i} u_0(x)] = f \tag{24}$$

Or, we return to the original scaling, we have that

$$-\nabla_x \cdot [A(\frac{x}{\varepsilon})(\vec{e_i} + \nabla w_i(\frac{x}{\varepsilon}))\partial_{x_i} u_0(x)] = f(x) \tag{25}$$

Since, as $\varepsilon \to 0$,using lemma 5.1

$$A(\frac{x}{\varepsilon})(\vec{e_i} + \nabla w_i(\frac{x}{\varepsilon})) \to \fint_Y A(y)(\vec{e_i} + \nabla w_i(y))dy \tag{26}$$

Since u_0 and f are independent of ε, we can conclude the homogenized problem component-wise:

$$-\nabla_x \cdot [\fint_Y A(y)(\vec{e_i} + \nabla w_i(y))dy\ \partial_{x_i} u_0(x)] = f(x) \tag{27}$$

We can very naturally deduce the homogenized coefficient A^{hom} as follows: for each $i = 1, 2, ..., N$, we define

$$\begin{aligned} &A^{hom} \cdot \vec{e_i} = \fint_Y A(y)(\vec{e_i} + \nabla w_i(y))dy \\ &\text{so that} A^{hom}_{ij} = \fint_Y A(y)(\vec{e_i} + \nabla w_i(y)) \cdot (\vec{e_j} + \nabla w_j(y))dy \end{aligned} \tag{28}$$

And conclude from the equation (27) that u_0 in asymptotic expansion solves the homogenized problem:

$$\begin{cases} -\nabla \cdot (A^{hom}(x)\nabla u_0(x)) = f(x) & in\ \Omega, \\ u_0 = 0 & on\ \partial\Omega. \end{cases} \tag{29}$$

3.4 Main Result in N-D Periodic PDE Coefficients

This theorem comes from [6].

Theorem 3.1. *For boundary value problem:*

$$\begin{cases} -\nabla \cdot (A(x, \frac{x}{\varepsilon})\nabla u_\varepsilon) = f & in\ \Omega, \\ u_\varepsilon = 0 & on\ \partial\Omega. \end{cases} \tag{30}$$

The sequence $u_\varepsilon(x)$ of solution for (30) converges weakly in $H^1_0(\Omega)$ to a limit $u(x)$ which will be the unique solution to the homogenized problem,

$$\begin{cases} -\nabla \cdot (A^{hom}(x)\nabla u(x)) = f(x) & in\ \Omega, \\ u = 0 & on\ \partial\Omega. \end{cases} \tag{31}$$

In (31), the homogenized diffusion tensor,A^{hom} is defined by entries as follows:

$$A^{hom}_{i,j}(x) = \fint_Y A(x,y)(\vec{e_i} + \nabla_y w_i(x,y)) \cdot (\vec{e_j} + \nabla_y w_j(x,y))dy, \tag{32}$$

where $w_j(x,y)$ are so-called homogenization correctors, as the unique solutions at each point $x \in \Omega$ of the corrector equation or cell problems:

$$\begin{cases} -\nabla_y \cdot (A(x,y)(\vec{e_i} + \nabla_y w_i(x,y))) = 0 & in\ Y, \\ y \to w_i(x,y) & Y-periodic. \end{cases} \tag{33}$$

with $(e_i)_{1 \le i \le N}$, the canonical basis of $\mathbb{R}^N$

3.5 Intuitive Proof of Convergence

To give some intuitive insight of the oscillating test function method, we begin a naive attempt to prove the main result Theorem 3.1 by passing the limit $\varepsilon \to 0$ in the weak solution of the boundary value problem.

$$\int_\Omega A_\varepsilon(x)\nabla u_\varepsilon(x) \cdot \nabla\phi(x)dx = \int_\Omega f(x)\phi(x)dx$$

for any test function $\phi \in H_0^1(\Omega)$. By the priori bound given in Lemma 3.1, we can construct a sequence u_ε which converges weakly to a limit u, but the left hand side of the weak solution above involves the product of two weakly convergent sequences in $L^2(\Omega)$, $A(x, \frac{x}{\varepsilon})$ and $\nabla u_\varepsilon(x)$, which is not convergent to the product of limits. So we cannot naively give the limiting result without any further argument.

This is where the oscillating test function takes place: we replace the fixed test function ϕ with a sequence ϕ_ε which is weakly convergent. The study on that oscillating test function will show that it is possible to take the limit on the left hand side of the weak solution using ϕ_ε and hence we can get the homogenized problem by taking the limit.

Proof. From Ulrich's book[6], the oscillating test function is defined :

$$\phi_\varepsilon(x) = \phi(x) + \varepsilon \sum_{i=1}^{N} \frac{\partial\phi}{\partial x_i} w_i^*(x, \frac{x}{\varepsilon}) \tag{34}$$

where $w_i^*(x, y)$ are not the solutions of the cell problems introduced before, but instead, the dual cell problems:

$$\begin{cases} -\nabla_y \cdot [A^t(x,y)(\vec{e_i} + \nabla_y w_i^*(x,y))] = 0 & \textit{in } Y, \\ y \to w_i^*(x,y) & Y - \textit{periodic} \end{cases} \tag{35}$$

The next step is to insert this function ϕ_ε into the weak solution of the original equation:

$$\int_\Omega A_\varepsilon(x)\nabla u_\varepsilon(x) \cdot \nabla\phi_\varepsilon(x)dx = \int_\Omega f(x)\phi_\varepsilon(x)dx \tag{36}$$

For ϕ_ε,

$$\begin{aligned} \nabla\phi_\varepsilon = &\sum_{i=1}^{N} \frac{\partial\phi}{\partial x_i}(x)(\vec{e_i} + \nabla_y w_i^*(x, \frac{x}{\varepsilon})) \\ &+ \varepsilon \sum_{i=1}^{N} (\frac{\partial\nabla\phi}{\partial x_i}(x) w_i^*(x, \frac{x}{\varepsilon}) + \frac{\partial\phi}{\partial x_i}(x)\nabla_x w_i^*(x, \frac{x}{\varepsilon})), \end{aligned} \tag{37}$$

Using Green's first identity on the left hand side of the equation (36), we have:

$$\begin{aligned} &\int_\Omega A(x, \frac{x}{\varepsilon})\nabla u_\varepsilon(x) \cdot \nabla\phi_\varepsilon(x)dx \\ &= \int_\Omega A(x, \frac{x}{\varepsilon})\nabla u_\varepsilon(x) \cdot \sum_{i=1}^{N} \frac{\partial\phi}{\partial x_i}(x)\left(\vec{e_i} + \nabla_y w_i^*(x, \frac{x}{\varepsilon})\right)dx \\ &+ \varepsilon \int_\Omega A(x, \frac{x}{\varepsilon})\nabla u_\varepsilon(x) \cdot \sum_{i=1}^{N} \left(\frac{\partial\nabla\phi}{\partial x_i}(x) w_i^*(x, \frac{x}{\varepsilon}) + \frac{\partial\phi}{\partial x_i}(x)\nabla_x w_i^*(x, \frac{x}{\varepsilon})\right)dx. \end{aligned} \tag{38}$$

Look at the last term of the right hand side of (38), it is bounded by a constant time and, thus, will cancel when takes the limit. In the first term, using Green's first identity once again, we have:

$$\begin{aligned} &\int_\Omega A(x, \frac{x}{\varepsilon})\nabla u_\varepsilon(x) \cdot \sum_{i=1}^{N} \frac{\partial\phi}{\partial x_i}(x)\left(\vec{e_i} + \nabla_y w_i^*(x, \frac{x}{\varepsilon})\right)dx \\ &= -\int_\Omega u_\varepsilon(x)\nabla \cdot \left(A^t(x, \frac{x}{\varepsilon})\sum_{i=1}^{N} \frac{\partial\phi}{\partial x_i}(x)\left(\vec{e_i} + \nabla_y w_i^*(x, \frac{x}{\varepsilon})\right)\right)dx. \end{aligned} \tag{39}$$

To simplify the equation, we compute the divergence, which is actually a function of x and $y = x/\varepsilon$:

$$
\begin{aligned}
div_\varepsilon(x) &:= \nabla \cdot \left(A^t(x, \frac{x}{\varepsilon}) \sum_{i=1}^{N} \frac{\partial \phi}{\partial x_i}(x) \left(\vec{e_i} + \nabla_y w_i^*(x, \frac{x}{\varepsilon}) \right) \right) \\
&= \nabla_x \cdot \left(A^t(x, y) \sum_{i=1}^{N} \frac{\partial \phi}{\partial x_i}(x)(\vec{e_i} + \nabla_y w_i^*(x, y)) \right) \\
&+ \frac{1}{\varepsilon} \sum_{i=1}^{N} \frac{\partial \phi}{\partial x_i}(x) \nabla_y \cdot \left(A^t(x, y)(\vec{e_i} + \nabla_y w_i^*(x, y)) \right)
\end{aligned}
\tag{40}
$$

Noticed that the ε^{-1} term is 0 by the definition of dual cell problem:

$$
\frac{1}{\varepsilon} \sum_{i=1}^{N} \frac{\partial \phi}{\partial x_i}(x) \nabla_y \cdot \left(A^t(x, y)(\vec{e_i} + \nabla_y w_i^*(x, y)) \right) = 0 \tag{41}
$$

Therefore,

$$
div_\varepsilon(x) = \nabla_x \cdot \left(A^t(x, y) \sum_{i=1}^{N} \frac{\partial \phi}{\partial x_i}(x)(\vec{e_i} + \nabla_y w_i^*(x, y)) \right) \tag{42}
$$

$div_\varepsilon(x)$ is bounded in $L^2(\Omega)$. And by lemma 5.1 again, we have the limiting value for $div_\varepsilon(x)$:

$$
\text{As } \varepsilon \to 0, div_\varepsilon(x) \text{ converges weakly to } \nabla_x \cdot \left(\fint_Y A^t(x, y) \sum_{i=1}^{N} \frac{\partial \phi}{\partial x_i}(x)(\vec{e_i} + \nabla_y w_i^*(x, y)) dy \right)
$$

Now, recall that u_ε is bounded (lemma 3.1), using Rellich theorem, there exists a subsequence and a limit $u \in H_0^1(\Omega)$ such that u_ε converges strongly to u in $L^2(\Omega)$. Hence now we can pass the limit $\varepsilon \to 0$ into the weak formulation.

$$
\lim_{\varepsilon \to 0} \int_\Omega A(x, \frac{x}{\varepsilon}) \nabla u_\varepsilon(x) \cdot \nabla \phi_\varepsilon(x) dx = - \int_\Omega u(x) \nabla_x \cdot \left(\fint_Y A^t(x, y) \sum_{i=1}^{N} \frac{\partial \phi}{\partial x_i}(x)(\vec{e_i} + \nabla_y w_i^*(x, y)) dy \right) dx. \tag{43}
$$

By our definition for the homogenized coefficient A^{hom} (28), it can be easily seen that right hand side of (43) is simply:

$$
- \int_\Omega u(x) \nabla \cdot \left((A^{hom})^t(x) \nabla \phi(x) \right) dx. \tag{44}
$$

Finally, using Green's first identity will yield back to the limiting formula:

$$
\int_\Omega A^{hom} \nabla u(x) \cdot \nabla \phi(x) dx = \int_\Omega f(x) \phi(x) dx. \tag{45}
$$

Notice that the equation (45) is valid for all test functions $\phi \in H_0^1(\Omega)$. And as the definition of A^{hom} indicates that A^{hom} also has the coerciveness and boundedness just as A in (12)), using Lax-Milgram Lemma, (45) will admit a unique solution in $H_0^1(\Omega)$. Therefore, this gives the convergence for any subsequences of u_ε to a same limit u. □

This completes the derivation for the convergence of u_ε under the definition of oscillating test function ϕ_ε, the most rigorous proof from scratch can be found in chapter 2 of [8] and chapter 2,3 of [9] Finally, the homogenization theory in N-D could finally be given just as Theorem (3.1).

The importance of this oscillating test function should be pointed out that this is a very general method in homogenization which does not require any specific geometric assumptions for the PDE coefficient of the system. It can also be used in much more complex PDE coefficient of the problem and the homogenization theory for N-D stochastic coefficient can also be developed using the very similar idea. To have some further study on it, see [8]. This finishes the N-D theory for periodic homogenization, and in the next section, we focus on how numerical solutions can help us to analyze the homogenization process.

4 Numerical verification of the theory in 2-D

Here we demonstrate homogenization in 2-D in the context of electrical conductor networks. However, similar techniques could be deployed in other fields satisfying the diffusion equation. Pseudo-codes are presented in this section. All relevant files, including source code and graphs plotted by Python, are available in the GitHub repository

This section is **NOT** a rigorous proof, but more of a heuristic illustration of one aspect of the theory. We aim to use numerical scheme on Python to plot our solution of different sub-problems for the following purposes:

- Provide a heuristic understanding of the problem
- Present a numerical validation of the theory
- Explore problems with no explicit solution or beyond Year 2 syllabus

4.1 Iterative Stencil Loop Method

4.1.1 Setting of the Problem

Consider a $N \times N$ square lattice of conductor plate of fixed unit area. Shown below are examples when $N = 8$. Here each square is made of material with electrical conductivity coefficient matrix satisfying regularity condition. At position $x = (i, j)$, denote its conductivity coefficient matrix as $a^N_{i,j}$, and its electric potential as $u^N_{i,j}$. Suppose there are two different types of materials in different colours, with different conductivity coefficient matrix.

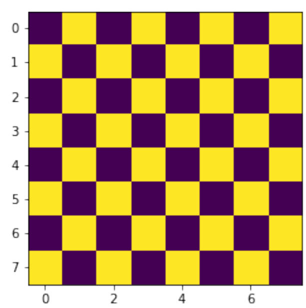

Figure 1: 8×8 Periodic distribution

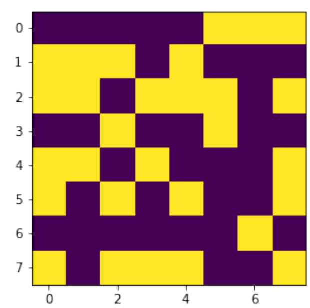

Figure 2: 8×8 stochastic distribution

The arrangement of two materials could be periodic or stochastic. In Figure 1, an illustration of periodic distribution is presented. In Figure 2, an illustration of stochastic distribution is presented. Notice the total area occupied by the two materials respectively are the same in both cases.

We impose the Dirichlet boundary condition. Apply an electric source in the centre and keep the voltage at the boundaries constant at zero. The size of the domain of source is in proportion to the grid size, hence unaffected by the increment of N. In the following subsections, we will observe homogenization via the convergence of u^N as N increases, in the steady-state of the electrical potential evolution.

4.1.2 Numerical Scheme

When increasing N, we see increasing frequency of oscillation of $a_{i,j}^N$. For simplicity, we assume $a_{i,j}^N$ is the same for squares in the same color. For periodic distribution, we define:

$$a_{i,j}^N = \begin{cases} \begin{pmatrix} 1 & 1 \\ 1 & 10 \end{pmatrix} & \text{if } i+j \equiv 0 \; mod \; 2 \\ \begin{pmatrix} 20 & 1 \\ 1 & 1 \end{pmatrix} & \text{if } i+j \equiv 1 \; mod \; 2 \end{cases}$$

We can see $a_{i,j}^N$ will only depend on i and j. In stochastic case, each square is randomly assigned to one of the coefficient matrices with equal probability(see Appendix for different probability ratio). These two specific coefficient matrices are chosen to best demonstrate homogenization visually. In Section 5.2, we will alter them and observe the corresponding influences. Notice here, $a_{i,j}^N$ is a 2×2 matrix, where the entries are denoted by $[a_{i,j}^N]_{kl}$. We can expand equation (13) as below.

$$\nabla \cdot (a_{i,j}^N \nabla u^N) + f = 0 \implies \sum_{l=1}^{2} \sum_{k=1}^{2} [a_{i,j}^N]_{kl} \partial_k \partial_l u^N + \sum_{l=1}^{2} \sum_{k=1}^{2} \partial_l([a_{i,j}^N]_{kl} \partial_k u^N) + f = 0$$

$$\begin{aligned} &[a_{i,j}^N]_{11} \partial_x \partial_x u^N + \partial_x [a_{i,j}^N]_{11} \partial_x u^N + \\ &[a_{i,j}^N]_{21} \partial_x \partial_x u^N + \partial_x [a_{i,j}^N]_{21} \partial_x u^N + \\ &[a_{i,j}^N]_{12} \partial_x \partial_x u^N + \partial_x [a_{i,j}^N]_{12} \partial_x u^N + \\ &[a_{i,j}^N]_{22} \partial_x \partial_x u^N + \partial_x [a_{i,j}^N]_{22} \partial_x u^N + f = 0 \end{aligned}$$

Under Schwarz integrability condition, we can interchange the order of partial differentiation. For any interior point in the lattice structure, it has four neighbouring points. At each point, $a_{i,j}^N$ is a known designated matrix. We can use central difference to approximate the partial derivatives as followed:

$$\begin{aligned} \partial_x \partial_x u^N &\approx \frac{u_{i+1,j}^N - 2u_{i,j}^N + u_{i-1,j}^N}{(\Delta x)^2} \\ \partial_y \partial_y u^N &\approx \frac{u_{i,j+1}^N - 2u_{i,j}^N + u_{i,j-1}^N}{(\Delta y)^2} \\ \partial_x \partial_y u^N &\approx \frac{u_{i+1,j+1}^N - u_{i+1,j-1}^N - u_{i-1,j+1}^N + u_{i-1,j-1}^N}{4 \Delta x \Delta y} \end{aligned}$$

Now consider an elliptic problem. At steady-state, a domain in the centre is kept at a constant value and the boundaries are absorbing(kept at zero). By setting $f = 0$ and $\Delta x = \Delta y$, we can obtain the relationship between $u_{i,j}^N$ and its four neighbours:

$$u_{i,j}^N = \frac{[a_{i,j}^N]_{11}(u_{i+1,j}^N + u_{i-1,j}^N) + \frac{[a_{i,j}^N]_{12} + [a_{i,j}^N]_{21}}{4}(u_{i+1,j+1}^N - u_{i+1,j-1}^N - u_{i-1,j+1}^N + u_{i-1,j-1}^N) + [a_{i,j}^N]_{22}(u_{i,j+1}^N + u_{i,j-1}^N)}{2[a_{i,j}^N]_{11} + 2[a_{i,j}^N]_{22}} \tag{46}$$

If we wish to use finite difference method, we would need to construct a system of linear equations and attempt to solve with matrix linear algebra techniques. However, it will become increasingly difficult to explicitly write out the matrix form. For example, for a 8×8 grid, a 64×64 matrix needs to be constructed. Instead, we can use an iterative process and loop over all interior points, keeping the centre domain and boundary values constant, then obtain the stationary distribution of electrical potential[10]. First set up a $N \times N$ grid of initial guess for u. Then use relationship (46) to update the values of all interior points. This is achieved by looping over all rows and columns (omit row 1, row N, column 1, column N since they are the boundaries). After all interior point values are updated, source is applied to keep the centre domain at constant potential. All above procedures are iterated for a large number of time T to obtain the steady-state of the system. T is determined with **While** loops conditioning on differences between the last two iterates. By lemma 3.1, we know u is bounded, hence it is valid to stop iteration after time T.

4.1.3 Plots with increasing resolution

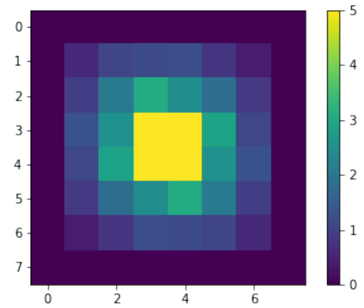

Figure 3: Periodic 8×8

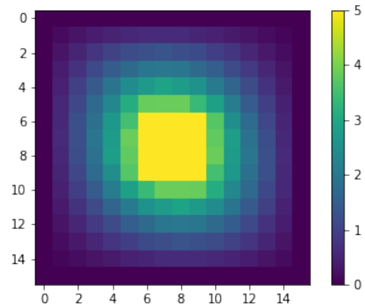

Figure 4: Periodic 16×16

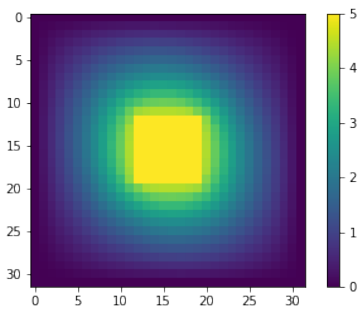

Figure 5: Periodic 32×32

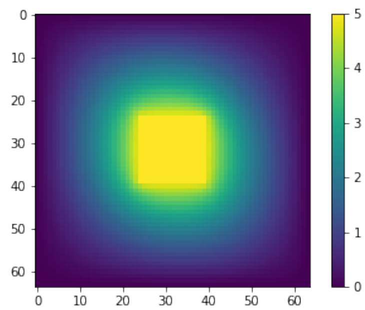

Figure 6: Periodic 64×64

As N increases, the unit area is being divided with an increasing number of squares. The heterogeneity varies on smaller microscale. Hence, N is inversely related to ε. Across Figure 3 to 6, periodic distribution in Figure 1 is adopted. As the number of grid points increases, the resolution increases, the images become smoother. Figure 6 looks as if it is produced with homogeneous material. Figure 7 is produced in a 64×64 grid with a homogeneous material with the conductivity coefficient $\begin{pmatrix} 20 & 1 \\ 1 & 10 \end{pmatrix}$ everywhere. Further work could be done to calculate $A_{i,j}^{hom}$ in equation (32) exactly and compare the images produced in theoretical results. However, visually we could see the similarities between Figure 6 and 7 and conclude our heterogeneous $a_{i,j}^{N}$ converges to a homogenized one.

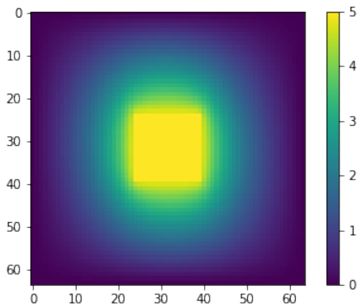

Figure 7: Homogeneous 64×64

Across Figure 8 to 11, stochastic distribution in Figure 2 is adopted. Comparing Figure 3 and Figure 8, we can see the randomness when the number of grid points is small. However, similar to the periodic distribution, as the number of grid points increases, the images become smoother. Heterogeneous materials appear to be homogeneous, supporting our theoretical result. Moreover, the elliptical shape agrees with the setting of the elliptical problem. Nevertheless Iterative Stencil Loop is not the only way to simulate the elliptical problem. Next, we will explore Relaxation method and see whether it produces similar results.

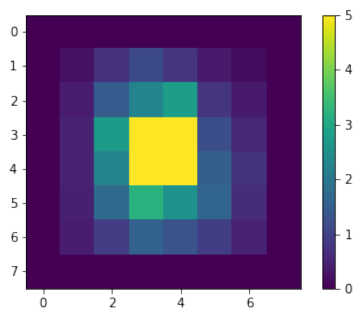

Figure 8: stochastic 8×8

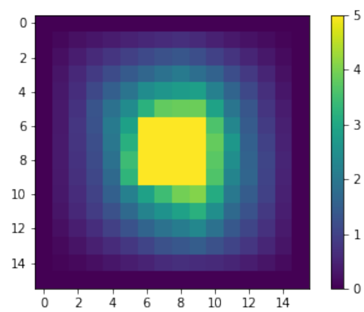

Figure 9: stochastic 16×16

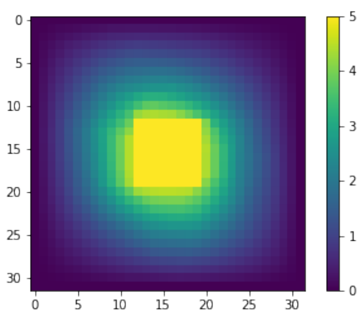

Figure 10: stochastic 32×32

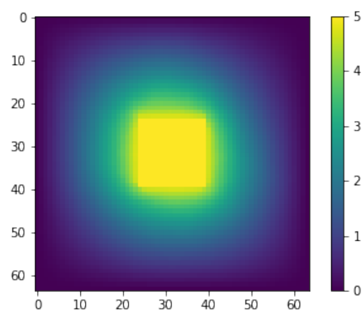

Figure 11: stochastic 64×64

4.2 Relaxation Method

4.2.1 Setting of the Problem

In this part we consider a discrete analogon of the problem, where finitely many "resistors" form a resistor network. Construction of this discrete model draws inspiration from [6]. We denote voltage at node n to be V_n, resistance between node n and central node to be R_n.

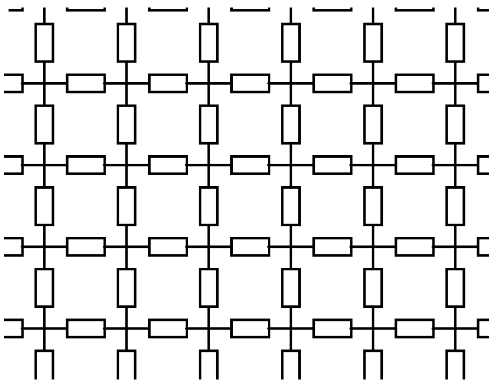

Figure 12: Resistor Network

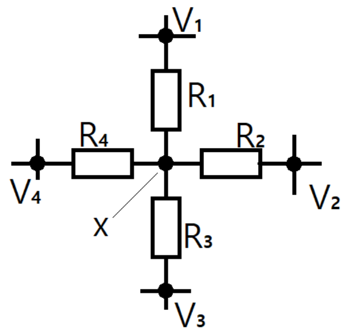

Figure 13: A node in network

The setting under 'circuit' does have the same essentials with the settings under heat conductivity. Note that when x is not in the source area, $\nabla \cdot (a\nabla u) = 0$ holds. This tells us that the net flux through a node outside source is zero, which means that:

$$\sum a_i(V_i - x) = 0$$

In circuit, it is convenient to use Kirchhoff's Current Law and Ohm's law to determine the coefficients a_i. Adopting the notation in Figure 13 gives the following:

$$\frac{x - V_1}{R_1} + \frac{x - V_2}{R_2} + \frac{x - V_3}{R_3} + \frac{x - V_4}{R_4} = 0$$

Rearranging the terms we obtain:

$$x = \frac{V_1(R_2R_3R_4) + V_2(R_1R_3R_4) + V_3(R_1R_2R_4) + V_4(R_1R_2R_3)}{(R_1R_2R_3 + R_1R_2R_4 + R_1R_3R_4 + R_2R_3R_4)} \tag{47}$$

which is the equation we will use for the method of relaxation in our numerical scheme.

4.2.2 Numerical Scheme

Under the assumption that time dependence can be omitted, we aim to seek for a steady-state of the problem. We set Ω to be a square plate with length 1, source region is located at the centre of the plate with length μ. Voltage is evaluated at each node connected as in Figure 12 by resistors, and resistor of certain resistance will be assigned according to setting of the problem.

For each iteration we shall first assign source values and boundary values in order to keep them constant. Then using equation (47) given above, we iterate over points outside source region by taking their weighted average.

In this context, function $a(x)$ takes position of the node i.e., where x is, as input, and outputs the resistance of the nodes' four nearby resistors, which is the "weight" in the average. For our programme, it is convenient to introduce an auxiliary matrix $P_{2m+1,m+1}$ to store the resistors information, we shall formulate our matrix P depending on the configuration of the newtork.

Finally, we denote result of k^{th} iteration to be U^k, which represents the value of $u(x)$ evaluated on the nodes. Set source strength to be 5 at each source node, we have:

$$U^0_{(i,j)} \begin{cases} 5 & \text{if in source} \\ 0 & \text{if not in source} \end{cases}$$

and

$$U^{k+1}_{(i,j)} \begin{cases} 5 & \text{if in source} \\ 0 & \text{if on boundary} \\ [U^k_{(i,j)}] & \text{otherwise} \end{cases}$$

where

$$\frac{[U^k_{(i,j)}] - U^k_{(i-1,j)}}{P_{(2i,j+1)}} + \frac{[U^k_{(i,j)}] - U^k_{(i+1,j)}}{P_{(2i+2,j+1)}} + \frac{[U^k_{(i,j)}] - U^k_{(i,j+1)}}{P_{(2i+1,j)}} + \frac{[U^k_{(i,j)}] - U^k_{(i,j-1)}}{P_{(2i+1,j-1)}} = 0$$

In the following sections,whenever this method is applied , we fix $\mu = 0.2$. In order to obtain the steady-state solution, we set iteration time N depending on grid number, hence the plots presented are be based on U^N under each problem settings.

For next section, we set our resistor network to have to following periodic structure: on each column and row of resistors, we arrange the resistance be be oscillating between 1 and R_x, where $R_x = 10$, as shown below.

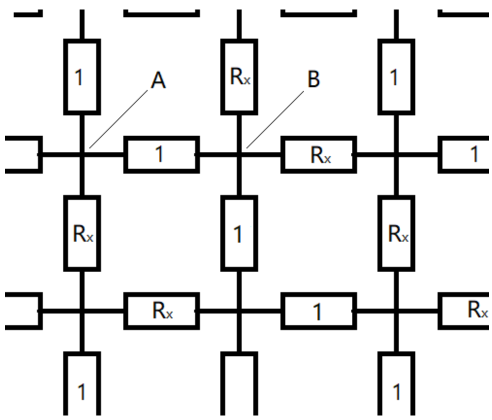

Figure 14: Resistor Network

For each node in the network, it would either be of type A or type B. In the programme this can be simply determined by deciding the parity of $i + j$ for node $U^k_{(i,j)}$, which simplifies the calculation for periodic case.

4.2.3 Plots with increasing resolutions

In this section we aim to observe how the decrease of ε changes our solution. This is achieved, in our numerical scheme, by increasing the grid number while preserving the relative size and position of the source. Plots below show the values of steady-state solution of u in Ω under four different resolutions. Complete set of images for this project including more plots on different resolutions are available on the project GitHub repository.

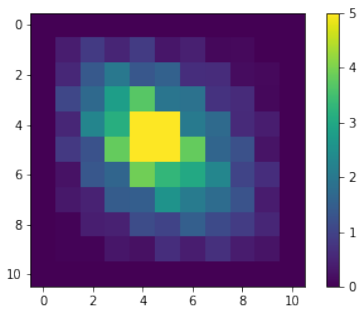

Figure 15: 11×11

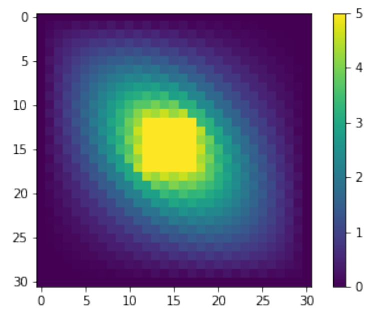

Figure 16: 31×31

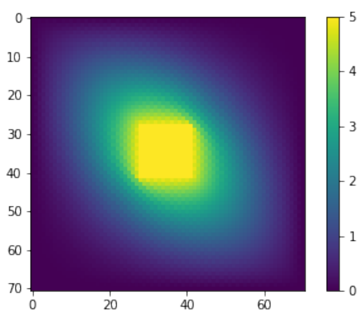

Figure 17: 71×71

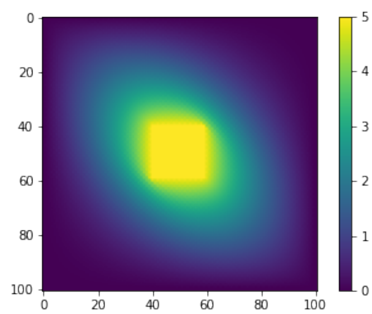

Figure 18: 101×101

Theory of homogenization predicts a smooth characteristic when taking ε to its limit of zero. We observe smoother characteristics which converge to elliptic shapes when resolution increases, which represents the convergence to the solution on a anisotropic homogeneous media. This agrees with the prediction of homogenization and also the result obtained by Iterative Stencil Loop.

4.2.4 Trend on sections

Here another perspective of the process is presented. Plots are given at certain y values to obtain behaviour of u^{ε} on 1-D 'sub-spaces' of Ω. y-axis represents value of u while x-axis marks x-coordinate, which is the distance from the point to the right-hand boundary counted in lattice number. The following plots are all presented with five different colour. Each color in the different plots represents the value of u at approximately the same physical space on the unit plate.

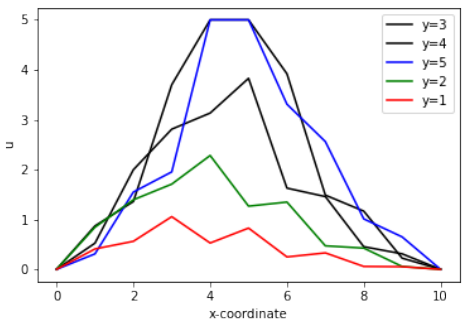

Figure 19: 11×11

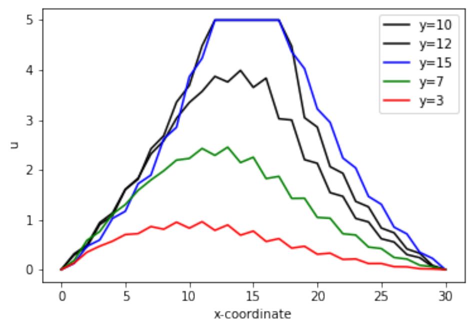

Figure 20: 33×33

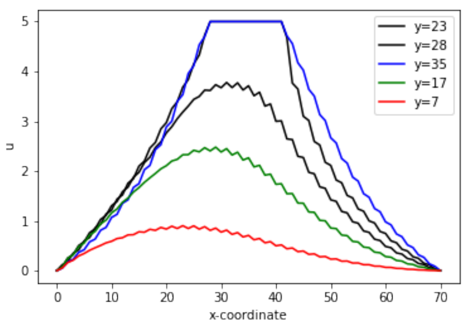

Figure 21: 71×71

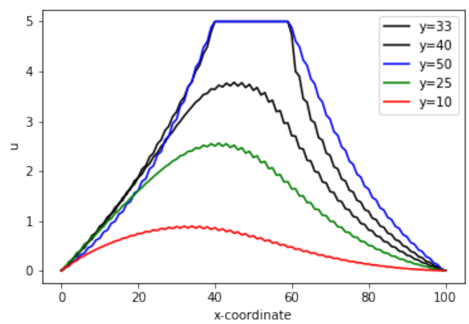

Figure 22: 101×101

First, the flat part of blue and black lines is the source area kept at a constant of 5 throughout the area. All values of u on both ends of the graphs are kept at zero, which is the boundary condition. We observe oscillation on each graph, representing the heterogeneous nature of the material on a microscopic scale. The amplitude of oscillations decreases with the increase of resolution, which again indicates convergence to a smooth function, showing a homogenized character on a macroscopic scale. This agrees with the theory of homogenization and the pictures presented in reference [6].

Secondly, we observe that with higher precision, the graphs tend to skewed 'Bell Curve', which is the characteristic shape of the steady-state solution of the heat equation. The skewness comes from the anisotropic character of the homogenized media. The curves are positively skewed since they are chosen on the same side of the source. However both positive and negative skewness occurs if lines are chosen on both different sides of the source. It is also inferred that given an isotropic media, no skewness will be observed(See Appendix for illustration).

4.2.5 Independence of $f(x)$

By theory of homogenization we expect our homogenization to be independent of $f(x)$. We could change the shape of the source and see a similar homogenized image. Here we present a simple case to illustrate this result intuitively. The rightmost figure presented is constructed in a similar way to Figure 19-22, but with all horizontal sections under the resolution plotted.

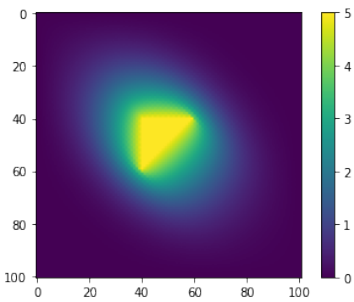

Figure 23: Triangular Source

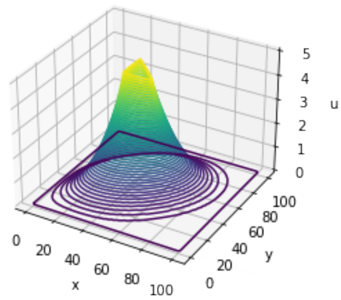

Figure 24: Triangular Source

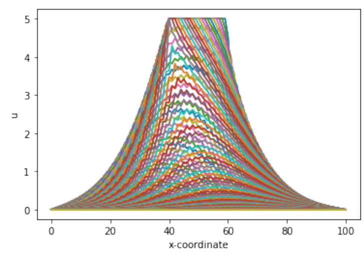

Figure 25: Triangular Source

We still observe characteristic of elliptic shape, which is skewed in the same direction as former one. We also notice that the skewness is similar to the one seen before, this agrees with the theory that process of homogenization is independent of $f(x)$ which tells us that we would expect same type of skewness on same setting of the network.

4.3 Remarks on the two methods

Iterative Stencil Loop uses finite central method to discretize the continuous equation (13) and obtains the discrete relation (46). When considering equation (13), explicit a_ε is defined. On the other hand, relaxation method considers a local problem and obtains equation (47). While a_ε is not displayed in the equation, it is implicitly incorporated by the structure of R_1, R_2, R_3 and R_4. Additionally, in defining the iterative process, both method utilizes Kirchhoff's Current Law, i.e., net flux through a node outside source is zero. The two iterative processes both act as a weighted average for any interior node and its four neighbors.

We can also see resemblance to numerical simulation solution to the Laplace Equation[2]. By setting off-diagonals in equation (46) to be zero and $R_1 = R_2 = R_3 = R_4$ in equation (47), standard averaging is obtained, which is the relationship between interior nodes and its four neighbors. Both methods are valid and produce similar plots which validate the theory of homogenization. As the number of grid points increases, ε decreases, and the images become smoother and suggest homogenization. They agree with our theoretical conclusion.

5 Applications

5.1 Layered Media

In this section, we first apply homogenization in N-D to calculate the effective property of a 2-D layered medium. The main results of this section come from Ulrich Hornung's book [6]. We then use the numerical simulation tools to investigate how different microstructures influence effective property.

5.1.1 Setting of the Problem

This section aims to calculate the effective parameters in a layered medium. We consider the diffusion process in a layered medium modelled by the following equation with $x \in \Omega = \{(x_1, x_2) : 0 < x_1, x_2 < 1\}$ in $\mathbb{R}^2$:

$$\nabla \cdot (a_\varepsilon(x)\nabla u_\varepsilon(x)) = 0 \tag{48}$$

As we are considering layered media, we assume that a_ε is a periodic function only depends on x_2 with periodicity length ε, i.e., we have

$$a_\varepsilon(x_1, x_2) = a\left(\frac{x_2}{\varepsilon}\right)$$

with $a : \mathbb{R} \to \mathbb{R}$ fixed and 1-periodic.

5.1.2 Find the effective property

We expect that the differential equation (48) homogenizes to

$$\nabla \cdot (A\nabla u_0) = 0 \tag{49}$$

with

$$A = \begin{pmatrix} \bar{a} & 0 \\ 0 & a^* \end{pmatrix}.$$

We consider the following two boundary problems to determine the numbers $\bar{a}$ and a^*.
Case 1. (Find $\bar{a}$)
Consider

$$\begin{cases} -\nabla \cdot [a(x)\nabla u(x)] = 0, & x \in \Omega \\ u = 0, & x_1 = 0 \\ u = 1, & x_1 = 1 \\ \partial_\nu u = 0, & x_2 = 0 \text{ or } x_2 = 1 \end{cases} \tag{50}$$

where ν is the outwards normal on $x_2 = 0$ or $x_2 = 1$.
Claim: $u(x_1, x_2) = x_1$ is a solution to (50).
Proof of claim: From $\nu = (0, \pm x_2)$, we have

1. $\partial_{x_2} u = 0 \Rightarrow \partial_\nu u = 0$
2. $u = 0$ when $x_1 = 0$ and $u = 1$ when $x_1 = 1$
3. $-\nabla \cdot [a(x)\nabla u(x)] = -\nabla \cdot [a(x)\vec{e_1}] = \partial x_1 a(x_2) = 0, \because$ a only depends on x_2

$\Rightarrow u(x) = x_1$ solves (50).

Claim: $u_\varepsilon(x_1 x_2) = x_1$ is a solution to rescaled problem:

$$\begin{cases} -\nabla \cdot [a_\varepsilon(x)\nabla u_\varepsilon(x)] = 0, & x \in \Omega \\ u_\varepsilon = 0, & x_1 = 0 \\ u_\varepsilon = 1, & x_1 = 1 \\ \partial_\nu u_\varepsilon = 0, & x_2 = 0 \text{ or } x_2 = 1 \end{cases} \tag{51}$$

Proof of claim: From $\nu = (0, \pm x_2)$, we have

1. $\partial_{x_2} u_\varepsilon = 0 \Rightarrow \partial_\nu u_\varepsilon = 0$
2. $u_\varepsilon = 0$ when $x_1 = 0$ and $u_\varepsilon = 1$ when $x_1 = 1$
3. $-\nabla \cdot [a_\varepsilon(x)\nabla u_\varepsilon(x)] = -\nabla \cdot (a_\varepsilon(x)\vec{e_1}) = \partial x_1 a\left(\frac{x_2}{\varepsilon}\right) = 0,\ \because a$ only depends on $\frac{x_2}{\varepsilon}$

$\Rightarrow u_\varepsilon(x) = x_1$ solves (51).

Therefore, the flux through the square, $a_\varepsilon \nabla u_\varepsilon$ satisfies

$$a_\varepsilon \nabla u_\varepsilon = a_\varepsilon \vec{e_1}$$

Then, we find the total flux through the square in x_1 direction by projecting to this direction first :

$$\begin{aligned} \int_0^1 a_\varepsilon \vec{e_1} \cdot \nabla u_\varepsilon dx_2 &= \int_0^1 a_\varepsilon(x_2)\, dx_2, \text{ as } \vec{e_1} \cdot \nabla u_\varepsilon = \begin{pmatrix} 1 & 0 \end{pmatrix} \cdot \begin{pmatrix} 1 & 0 \end{pmatrix} = 1 \\ &= \int_0^1 a(\eta) d\eta \end{aligned}$$

As the total flux of the homogenized case (49) is $\bar{a}$ and it should equal to the flux in the rescaled case. Therefore, we conclude that $\bar{a} = \int_0^1 a(\eta) d\eta$.

Case 2: (Find a^*)
Consider

$$\begin{cases} -\nabla \cdot [a(x)\nabla u(x)] = 0, & x \in \Omega \\ u = 0, & x_2 = 0 \\ u = 1, & x_2 = 1 \\ \partial_\nu u = 0, & x_1 = 0 \text{ or } x_1 = 1 \end{cases} \tag{52}$$

Using same method in case 1, we have $u(x_1, x_2) = x_2$ is a solution to (52).
Consider the rescaled problem:

$$\begin{cases} -\nabla \cdot [a_\varepsilon(x)\nabla u_\varepsilon(x)] = 0, & x \in \Omega \\ u_\varepsilon = 0, & x_2 = 0 \\ u_\varepsilon = 1, & x_2 = 1 \\ \partial_\nu u_\varepsilon = 0, & x_1 = 0 \text{ or } x_1 = 1 \end{cases} \tag{53}$$

By substituting $u_\varepsilon(x_1, x_2) = x_2$ into (53), we have

$$\nabla \cdot [a_\varepsilon(x)\nabla u_\varepsilon(x)] = \nabla \cdot \left[a\left(\frac{x_2}{\varepsilon}\right)\vec{e_2}\right] = \partial_{x_2} a\left(\frac{x_2}{\varepsilon}\right) \neq 0$$

therefore $u_\varepsilon(x) = x_2$ is not a solution to (53).
We then define $v =: u_\varepsilon - u_0$, with $u_0(x_1, x_2) = x_2$. The rescaled problem becomes:

$$\begin{cases} -\nabla \cdot [a_\varepsilon(x)\nabla v(x)] = 0, & x \in \Omega \\ v = 0, & x_2 \in \{0, 1\} \\ \partial_{x_1} v = 0, & x_1 \in \{0, 1\} \end{cases} \tag{54}$$

From the definition of v, we have

$$\begin{aligned} -\nabla \cdot [a_\varepsilon(x)\nabla v(x)] &= -\nabla \cdot [a_\varepsilon(x)\nabla (u_\varepsilon - u_0)] \\ &= -\nabla \cdot [a_\varepsilon(x)\nabla u_\varepsilon] + \nabla \cdot [a_\varepsilon(x)\nabla u_0], \text{ by linearity of } \nabla \\ &= \nabla \cdot [a_\varepsilon(x)\nabla u_0] \end{aligned}$$

Therefore,

$$-\nabla \cdot [a_\varepsilon(x)(\nabla v + \vec{e_2})] = 0.$$

Now consider δ, a 1-periodic solution to the following boundary problem:

$$\begin{cases} -\nabla \cdot a(x)\left(\nabla\delta + \vec{e}_2\right) = 0, & x \in \Omega \\ \delta = 0, & x_2 \in \{0,1\} \\ \partial_{x_1}\delta = 0, & x_1 \in \{0,1\} \end{cases} \tag{55}$$

$\because \delta = \delta(x_2)$, i.e., periodic in $x_2 \Rightarrow \partial_{x_1}\delta = 0 \Rightarrow \nabla\delta = \begin{pmatrix} 0 \\ \partial_{x_2}\delta \end{pmatrix}$.

Therefore, left to show that δ satisfies:

$$\begin{cases} -\partial_{x_2}\left(a(x)\left(\partial_{x_2}\delta + 1\right)\right) = 0, & x \in \Omega \\ \delta = 0, & x_2 \in \{0,1\} \end{cases} \tag{56}$$

Therefore,

$$\begin{aligned} a(x)\left(\partial_{x_2}\delta + 1\right) &= c,\ c \in \mathbb{R} \text{ is a constant} \\ \partial_{x_2}\delta &= \frac{c}{a(x)} - 1 \\ \delta &= \int_0^{x_2} \frac{c}{a(t)} - 1dt, \text{ as } \delta(0) = 0 \end{aligned}$$

To determine c :
From $\delta(1) = 0$, we have

$$\begin{aligned} \delta &= \int_0^1 \frac{c}{a(t)} - 1dt = 0 \\ \Rightarrow c &= \frac{1}{\int_0^1 \frac{1}{a(t)}dt} \\ \Rightarrow \delta &= a^* \int_0^{x_2} \frac{1}{a(t)}dt - x_2 \text{ with } a^* = \frac{1}{\int_0^1 \frac{1}{a(t)}dt} \end{aligned}$$

As v is the solution to the rescaled problem (54), we can rescale δ to get v:

$$v = \varepsilon\delta\left(\frac{x}{\varepsilon}\right)$$

Claim: v solves (54).
Proof of claim:

$$\begin{aligned} -\nabla \cdot \left[a_\varepsilon(x)\left(\nabla v(x) + \vec{e}_2\right)\right] &= -\nabla \cdot \left[a_\varepsilon(x)\begin{pmatrix} 0 \\ \partial_{x_2}\delta\left(\frac{x_2}{\varepsilon}\right) + 1 \end{pmatrix}\right] \\ &= 0, \text{ as } \delta \text{ satisfies (56).} \end{aligned}$$

As δ satisfies the boundary conditions in (55), v also satisfies the boundary conditions in (54).

As $v = u_\varepsilon - u_0$, we have

$$\begin{aligned} u_\varepsilon &= u_0\left(x_1, x_2\right) + v \\ &= u_0\left(x_1, x_2\right) + \varepsilon\delta\left(\frac{x_2}{\varepsilon}\right) \end{aligned}$$

with $u_0\left(x_1, x_2\right) = x_2$ and $\delta\left(y_2\right) = a^* \int_0^{y_2} \frac{d\eta}{a(\eta)} - y_2$.

Therefore, by Fundamental Theorem of Calculus, we have

$$a_\varepsilon \nabla u_\varepsilon = a_\varepsilon \nabla\left[x_2 + \varepsilon\left(a^* \int_0^{\frac{x_2}{\varepsilon}} \frac{dx_2'}{a(x_2')} - \frac{x_2}{\varepsilon}\right)\right] = a_\varepsilon\left(0, \frac{a^*}{a_\varepsilon}\right) = (0, a^*) = a^*\vec{e}_2 \text{ with } \vec{e}_2 = (0,1)$$

By considering the total flux through the square, we have

$$\int_0^1 a_\varepsilon \vec{e}_2 \cdot \nabla u_\varepsilon dx_1 = \int_0^1 a^* dx_1 = a^*.$$

We conclude that $a^* = \dfrac{1}{\int_0^1 \frac{1}{a(t)}dt}$.

5.2 Microscopic structures

In this section, we will continue using the numerical simulation tools to investigate how variations on microscopic structures changes the property of the homogenized media. Here we adopt the settings and notations of the resistor networks.

5.2.1 Layered Media

To model layered media, which is a set of special cases of periodic media, we adjust our setting of resistor network as shown below:

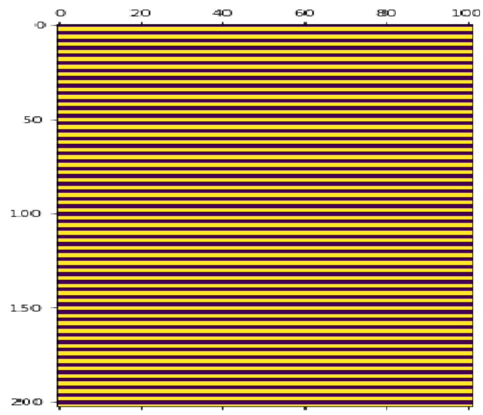

Figure 26: Layered Media

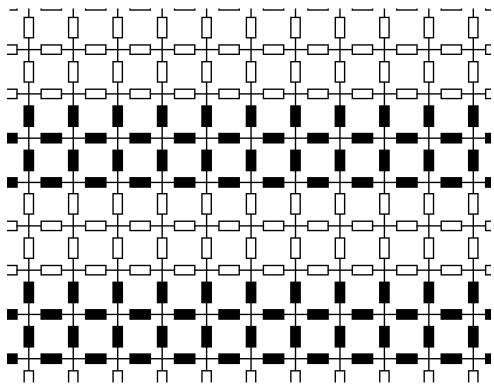

Figure 27: Network Configuration

For auxiliary matrix P we have that

$$P_{i,j} = P_{i,1} = \begin{cases} 1 & \text{if } \lfloor \frac{i}{4} \rfloor \text{ is odd} \\ R_x & \text{if } \lfloor \frac{i}{4} \rfloor \text{ is even} \end{cases}, \ \forall j = 1, 2.....n$$

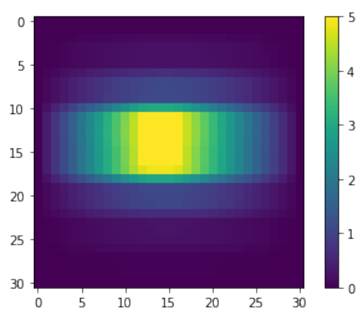

Figure 28: 31×31

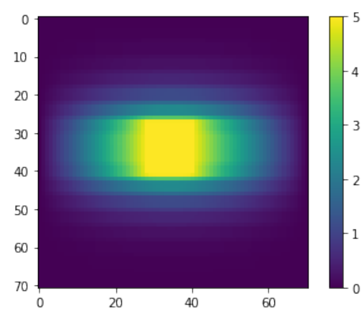

Figure 29: 71×71

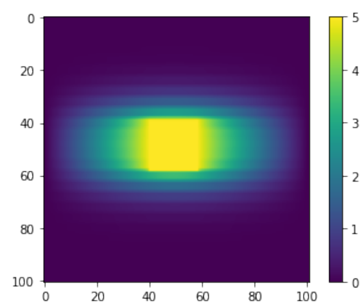

Figure 30: 101×101

We can compare three graphs given above, as resolution increases we observe trend of homogenization on layered media. By results of 5.1 we know that in vertical direction, the effective conductance is the harmonic average of the two media: $\frac{1}{1+1/r_x} = 1 + \frac{1}{R_x}$, while it is the arithmetic average of them horizontally: $\frac{1+R_x}{2}$.

We notice that voltage is more inclined to spread horizontally, and that the spread on decrease. An excellent analogy of layered media case would be resistors in series and in parallel, where harmonic average and arithmetic average are used in calculating effective conductance and effective resistance.

5.2.2 Stochastic

For simulation of stochastic media, **ALL** resistors in the network described in Figure 12 to have a random variable as resistance. Here using the multinomial distribution, we plot for two different configurations.

Configuration A:

$$P_{(R_x=1)} = 0.3, \; P_{(R_x=5)} = 0.7$$

Configuration B:

$$P_{(R_x=1)} = 0.3, \; P_{(R_x=10)} = 0.3, \; P_{(R_x=50)} = 0.4$$

Under the setting of resistor network we expect an isotropic media. This is because the value of resistance has no directional preference. Since the simulations are based on finitely many grids, we expect to observe "almost isotropic" character from the plots.

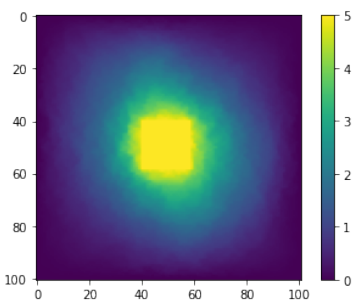

Figure 31: A

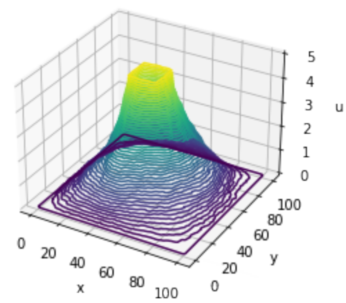

Figure 32: A

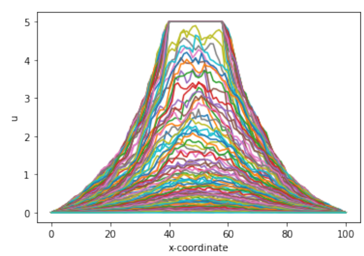

Figure 33: A

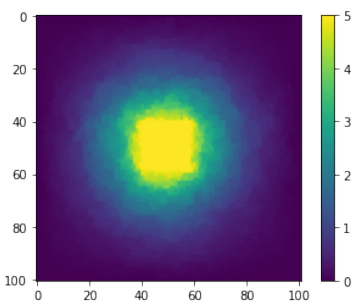

Figure 34: B

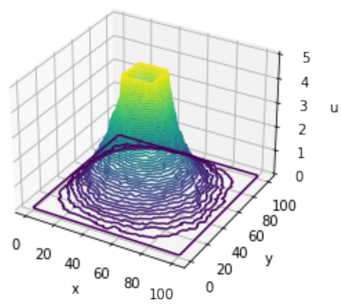

Figure 35: B

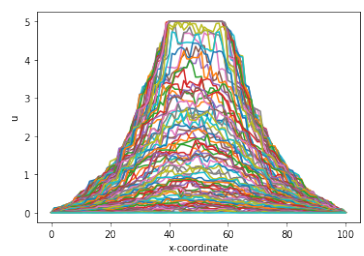

Figure 36: B

For case A, clear stochastic character is observed from the plots. From the leftmost pictures, we do not observe perfectly smooth character. "Almost circular" characters are observed, with stochastic oscillations, indicating an "almost isotropic" property of the homogenized media. From rightmost pictures, in case A, curves of shapes close to bell curves can still be observed, since the components are of very close resistance.

Informally and intuitively, plots for case B are "not very isotropic". We conjecture that this is due to the great change in resistance values as well as the fact that more resistance values are involved. When grid number is fixed, larger difference in media property can make it more difficult to show homogenization on the graph. This can be resolved by increasing the resolution of the grid. In material science, this may indicates that, the scale for a combination of two material structures with large difference in their property to show homogenization is larger than those that are small.

5.3 Further questions

So far we have been using the diffusion equation in the form of equation (1) and (13) and showed homogenization via the convergence of u_ε towards u_{hom}. However, homogenization could be observed in vastly different settings too. Consider a SIR model as below:

$$\begin{aligned}\frac{dS}{dt} &= -\frac{\beta S I}{N},\\ \frac{dI}{dt} &= \frac{\beta S I}{N} - \gamma I,\\ \frac{dR}{dt} &= \gamma I\end{aligned}$$

This is a simple mathematical description of the spread of a disease in a population of N individuals. An individual at time t is either susceptible, infectious or recovered (immune). Respectively, $S(t)$ are the individuals susceptible but not yet infected with the disease; $I(t)$ are the infectious individuals; $R(t)$ are those individuals who have recovered from the disease and now have immunity to it.

The SIR model describes the change in the population of each of three states in terms of two parameters: β and γ where β describes the effective contact rate of the disease and γ is the mean recovery rate.[5] However, this model assumes a homogenized β and γ across the population. It is more realistic to think there are subgroups within the population whose β and γ are different from one another. For instance, young people could have a higher recovery rate and elders might have higher contract rate of the disease. Within communities, there would be distribution of both young and elders. In a different light, we could view the entire population as a heterogeneous media where there are variations of transmissibility on the community (micro) scale. We might be able to observe homogenization in the spread of the disease on the macro (regional, national, and even global) scale. This means the disease spreads across the whole population as if it has a uniform contract and recovery rate. For example, we could examine the spread of COVID-19 in small communities and globally and determine the validity of homogenization theory in such context.

Appendix

1) Poincare's inequality (in 1-D)
First denote the norm on vector spaces of continuous functions $||u||_2$ and $|u||_\infty$, $\forall u \in C(0,1)$ by:

$$||u||_2 = \left(\int_0^1 u(x)^2 dx\right)^{1/2} ; ||u||_\infty \quad = \sup_{x\in(0,1)} |u(x)|$$

Claim: $\int_0^1 (u)^2 dx \leq \int_0^1 (u')^2\, dx$
Proof of Claim: Let $u(x) = \int_0^x u'(s)ds$, Then by some bounding, we have that

$$|u(x)| = \left|\int_0^x u'(s)ds\right| \leq \int_0^x \left|u'(s)\right| ds \leqslant \int_0^1 \left|u'(s)|ds\right.$$

Taking supremum on both sides, we have that:

$$||u||_\infty^2 \leqslant \left(\int_0^1 |u'(s)|ds\right)^2 \leq \left(\int_0^1 (u(s))ds\right)^2 \int_0^1 1ds = \left\|u'\right\|_2^2$$

Now we want to show that $||u||_2^2 \leqslant ||u||_\infty^2$:

$$||u||_2^2 = \int_0^1 |u(x)|^2 dx \leq \int_0^1 ||u||_\infty^2 dx = ||u||_\infty^2 \int_0^1 dx = ||u||_\infty^2$$

Thus, by joining the two inequalities we have:

$$\left\|u|_2\right.^2 \leqslant \left\| u \right\|_\infty^2 \leqslant \left\| u'\right||_2^2$$

which proves our claim by definition of $||.||_2$

2) Young's Inequality

$$ab \leq \frac{\delta}{2}a^2 + \frac{1}{20}b^2.$$

Prof: The expression is equivalent to

$$\forall \delta > 0 \text{ and } a, b \in \mathbb{R} : \frac{(\delta a - b)^2}{2\delta} \geq 0$$

$$\Leftrightarrow \quad \frac{\delta^2 a^2 - 2\delta ab + b^2}{2\delta} \geqslant 0 \Leftrightarrow \quad ab \leqslant \frac{\delta^2 a^2 + b^2}{2\delta} \Leftrightarrow \quad ab \leq \frac{\delta}{2}a^2 + \frac{1}{2}b^2$$

which proves the inequality.

3) Limit of weak convergence cell

Lemma 5.1. *Y is the periodic cell defined in section 3.*
Let w(x,y) be a continuous function in x, square integrable and Y-periodic in y. Then, as $\varepsilon \to 0$*, the sequence* $w(x, \frac{x}{\varepsilon})$ *converges weakly to* $⨍_Y w(x, y)dy$.

Proof. The proof can be found in the appendix of the article [4] □

4) Iterative Stencil Loop Method with Probability Ratio 1:3

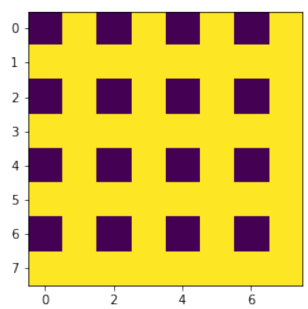

Figure 37: Periodic distribution

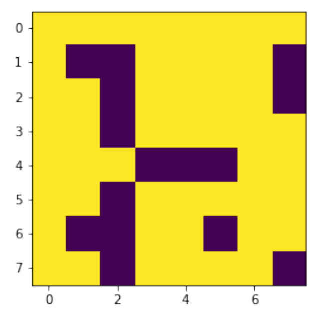

Figure 38: stochastic distribution

The same setting in 4.1.1 is considered. However, only a quarter of the total area is occupied by the purple material with conductivity coefficient matrix $\begin{pmatrix} 1 & 1 \\ 1 & 10 \end{pmatrix}$, the remaining area is occupied by yellow material with conductivity coefficient matrix $\begin{pmatrix} 20 & 1 \\ 1 & 1 \end{pmatrix}$, as depicted in Figure 45 and 46 in periodic and stochastic distribution. All other procedures are kept the same. Similar images are produced and we can infer that for different ratios the same conclusion could be reached: as the number of grid points increases, the images become smoother. Heterogeneous materials appear to be homogeneous, supporting our theoretical result. A different elliptical shape is observed, as expected.

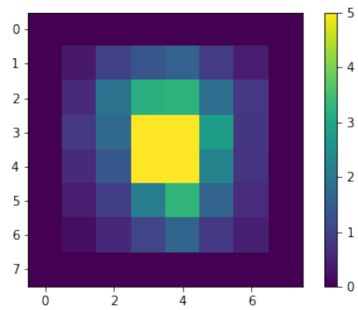

Figure 39: Periodic 8×8

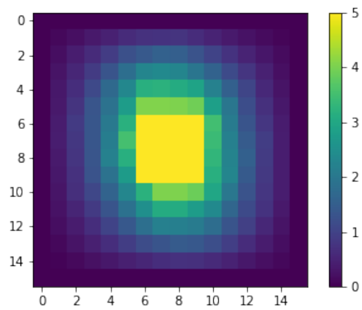

Figure 40: Periodic 16×16

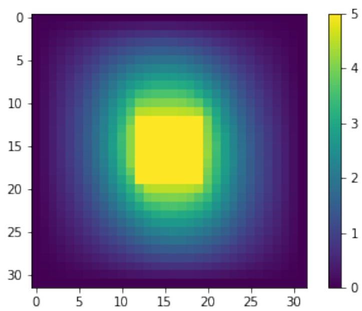

Figure 41: Periodic 32×32

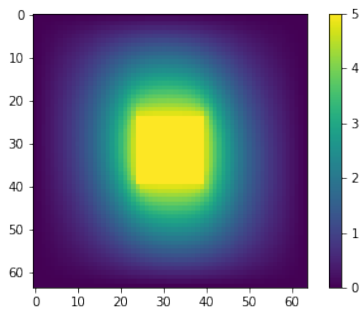

Figure 42: Periodic 64×64

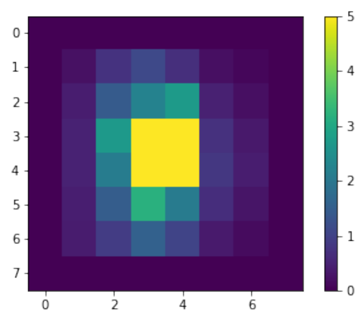

Figure 43: stochastic 8×8

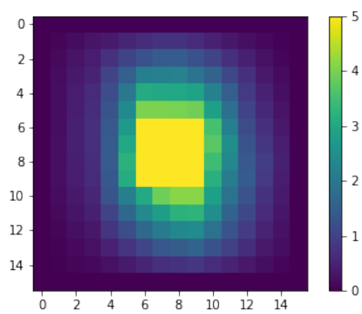

Figure 44: stochastic 16×16

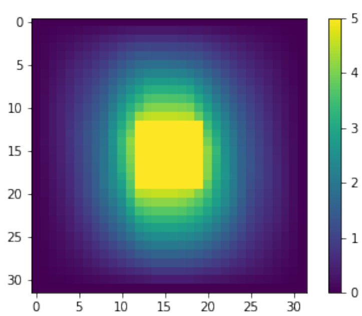

Figure 45: stochastic 32×32

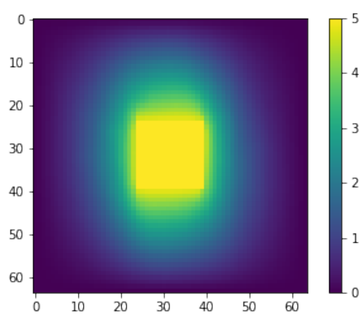

Figure 46: stochastic 64×64

5.3.1 Change of R_x in periodic case

In the previous sections we used networks as shown in the Figure 14. Now, by changing the value of R_x while preserving the structure, we observe a change in the steady solution.

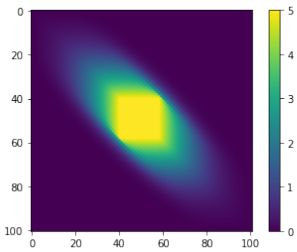

Figure 47: R=100

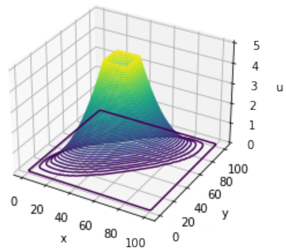

Figure 48: R=100

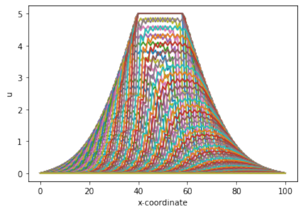

Figure 49: R=100

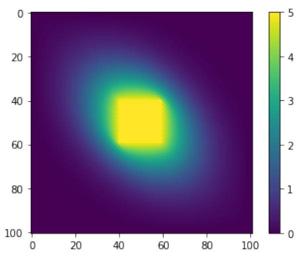

Figure 50: R=10

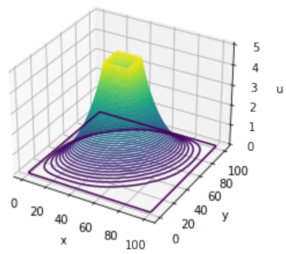

Figure 51: R=10

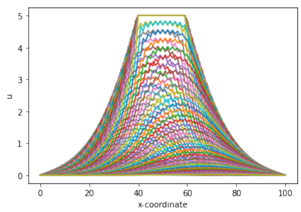

Figure 52: R=10

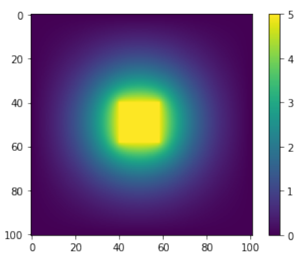

Figure 53: R=1

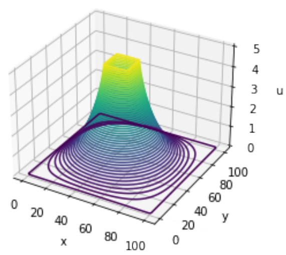

Figure 54: R=1

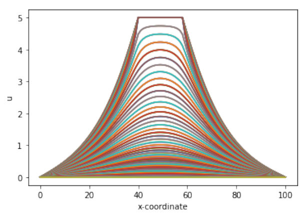

Figure 55: R=1

When $R = 1$ we observe isotropic character of the homogenized media. As R increases, the characteristics are more skewed, since the microscopic structure decides higher effective conductance on diagonal from top left to bottom right.

Through this case, we conclude that to change the directional preference of conductivity, one can, in some case, simply achieve this by changing one component of the composite.

References

[1] Alen Alexanderian. "A brief note on stochastic homogenization in 1D". In: (July 2013).

[2] Muhammadjamil Amir, Muhammad Yaseen, and Rabia Iqbal. "Exact solutions of Laplace equation by differential transform method". In: (Dec. 2013).

[3] Guillaume Bal et al. "Random integrals and correctors in homogenization". In: *Asymptotic Analysis* 59 (Jan. 2008). DOI: 10.3233/ASY-2008-0890.

[4] J.M Ball and F Murat. "W1,p-quasiconvexity and variational problems for multiple integrals". In: *Journal of Functional Analysis* 58.3 (1984), pp. 225–253. ISSN: 0022-1236. DOI: https://doi.org/10.1016/0022-1236(84)90041-7. URL: https://www.sciencedirect.com/science/article/pii/0022123684900417.

[5] Christian Hill. *Learning Scientific Programming with Python*. Cambridge University Press, 2016. DOI: 10.1017/CBO9781139871754.

[6] Ulrich Hornung. *Homogenization and porous media*. eng. Interdisciplinary applied mathematics ; 6; Pages 8-12,233-247. New York ; Springer, 1997. ISBN: 0387947868.

[7] Bienvenido Barraza Martínez, Jonathan González Ospino, and Jairo Hernández Monzón. *On Trace Theorems and Poincare inequality for one-dimensional Sobolev spaces*. 2021. DOI: 10.48550/ARXIV.2108.13926. URL: https://arxiv.org/abs/2108.13926.

[8] Stefan Neukamm. *An introduction to the qualitative and quantitative theory of homogenization*. 2017. DOI: 10.48550/ARXIV.1707.08992. URL: https://arxiv.org/abs/1707.08992.

[9] Christophe Prange. "Lecture 1: The Oscillating Test Function Method". In: 2016. URL: https://prange.perso.math.cnrs.fr/documents/coursEDMI2016_lecture1.pdf.

[10] Gerald Roth et al. "Compiling Stencils in High Performance Fortran". In: *In Supercomputing '97: Proceedings of the 1997 ACM/IEEE conference on Supercomputing (CDROM*. ACM Press, 1997, pp. 1–20.

[11] Luc Tartar. "Compensated compactness and applications to partial differential equations". In: *Nonlinear analysis and mechanics: Heriot-Watt symposium*. Vol. 4. 1979, pp. 136–212.

[12] Luc Tartar. "H-measures, a new approach for studying homogenisation, oscillations and concentration effects in partial differential equations". In: *Proceedings of the Royal Society of Edinburgh: Section A Mathematics* 115.3-4 (1990), pp. 193–230. DOI: 10.1017/S0308210500020606.

[13] Luc Tartar. "Incompressible fluid flow in a porous medium-convergence of the homogenization process". In: *Appendix of Non-homogeneous media and vibration theory* (1980).